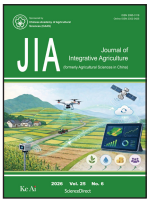
Journal of Integrative Agriculture 2026, 25(6): 2414–2433

Available online at ScienceDirect

Journal of Integrative Agriculture



RESEARCH ARTICLE

Epigenomic regulation of flowering in apple: Insights from two contrasting cultivars

Jiahui Song[1*], Lin Li[1*], Jiahe Wang[1*], Yuqing Xia[1], Heyu Zhang[1], Jingwen Li[1], Juanjuan Ma[1], Dong Zhang[1], Jiangping Mao[1], Na An[2], Libo Xing[1#]

[1] *College of Horticulture, Northwest A&F University, Yangling 712100, China*
[2] *College of Life Sciences, Northwest A&F University, Yangling 712100, China*

Highlights

- 'Qinguan' and 'Fuji' have completely opposite axillary bud flowering behaviors.
- DNA methylation plays an important role in the regulation of axillary bud flowering.
- DNA methylation of genes in plant hormone synthesis contributes to axillary bud flowering.

Abstract

Flowering is a necessary condition and basis for yield in the life cycle of woody fruit trees. Although there has been considerable interest in the regulatory mechanisms underlying floral induction and flowering, the associated epigenetic modifications remain poorly characterized. We identified genome-wide DNA methylation changes and the transcriptional responses in axillary buds of 'Qinguan' (QA) and 'Fuji' (FA) varieties with contrasting flowering behaviors. The DNA methylation levels were 19.35, 62.96 and 17.68% in FA, and 19.64, 62.49 and 17.86% in QA in the CG, CHG and CHH contexts, respectively. The number of hypermethylated and hypomethylated differentially methylated regions (DMRs) in different regions contributed to significantly up- and downregulated gene expression. DNA methylation can positively or negatively regulate gene expression depending on the CG, CHG and CHH contexts and their locations in different regions. Additionally, the huge differences in transcription of MIKC^{c}-type *MADS-box* genes, and multiple flowering genes in multiple flowering pathways (i.e., light, aging, GA and sugar) by changing DNA methylation, contributed to contrasting flowering behaviors in both QA and FA. Specifically, the floral meristem identity genes (i.e., *FT*, *LEAFY*, *AP1* and *SOC1*) exhibited significantly higher expression in QA than FA, but the floral repressors (i.e., *SVP*, *AGL15*, and *AGL18*) showed the opposite trend. Significant differences in multiple hormone levels were due to differentially expressed genes (DEGs) and their DMRs in hormone synthesis pathways, leading to both contrasting axillary bud outgrowth and flowering behaviors. These findings reflect the diversity in the epigenetic regulation of gene expression and may be helpful for elucidating the epigenetic regulatory mechanism underlying the axillary bud flowering in apple.

Keywords: apple trees, DMRs, RNA sequencing, axillary bud flowering, DNA methylation

1. Introduction

China's apple production still ranks first in the world, accounting for 57.4% of the world's total output (FAO 2023). However, the apple industry still faced some key production problems with poor-quality flower buds, and alternate bearing. This is especially true for the 'Fuji' variety, which accounts for more than 65% of the total cultivated area in China (Xing *et al.* 2016b, 2019a, b). Additionally, different varieties, i.e., profusely flowering 'Qinguan' (QA) and weakly flowering 'Fuji' (FA) (Haberman *et al.* 2016; Chen *et al.* 2018), as well as different types of shoots lead to diverse flowering capabilities, indicating that flower induction in woody fruit trees is a more complicated regulatory process influenced by multiple factors (Xing *et al.* 2016a, 2019a, b). Although studies on regulatory

Received 13 November 2024; Received in revised form 8 April 2025; Accepted 25 September 2025; Available online 31 December 2025
Jiahui Song, E-mail: 2542590209@qq.com; Lin Li, E-mail: 1957491233@qq.com; Jiahe Wang, E-mail: 1028925699@qq.com; #Correspondence Libo Xing, E-mail: libo_xing@nwafu.edu.cn
* These authors contributed equally to this study.

© 2026 CAAS. Publishing services by Elsevier B.V. on behalf of KeAi Communications Co. Ltd. This is an open access article under the CC BY-NC-ND license (http://creativecommons.org/licenses/by-nc-nd/4.0/). Peer review under responsibility of Editorial Board of *Journal of Integrative Agriculture*.
doi: 10.1016/j.jia.2025.12.065

mechanisms and networks of flowering in woody fruit trees have been reported (Albani and Coupland 2010; Xing L B *et al.* 2015; Haberman *et al.* 2016), little is still known regarding the molecular regulatory mechanisms of floral induction involving epigenetic modification in apple trees.

Cytosine methylation (DNA methylation) as one of the regulatory mechanisms of epigenetic modification plays key roles in the regulation of multiple life processes in plants, such as flower induction and flower development (Xing *et al.* 2019a), juvenile-to-adult transition (Kim *et al.* 2015; Xu *et al.* 2016), germination (Narsai *et al.* 2017), reproductive development (Han *et al.* 2019), and fruit development and ripening (Seymour *et al.* 2008; Liu *et al.* 2015; Gallusci *et al.* 2016). Additionally, DNA methylation can positively or negatively regulate gene expression based on the regions where methylation occurs, involving CG, CHG and CHH contexts in multiple woody plants, such as apple (Xing *et al.* 2019a), pear (Wang *et al.* 2013), and citrus (Xu *et al.* 2015; Agustí *et al.* 2020).

Now, the model plant, *Arabidopsis thaliana*, has evolved six major flowering regulatory pathways, i.e., photoperiod, vernalization, autonomous, gibberellic acid (GA), thermosensory and aging, to regulate flowering under internal and various environmental signal conditions (Amasino and Michaels 2010; Andrés and Coupland 2012; Xing M Q *et al.* 2015; Jung 2017). In this process, some key flowering genes including *FT*, *SOC1*, *LEAFY*, and *AP1*, act as floral integratiors and play key roles in regulating flowering, involving in mRNA transcription and epigenetic regulation (Dorca-Fornell *et al.* 2011; Qin *et al.* 2017; Zicola *et al.* 2019). For example, the expression of *FT* gene is regulated by epigenetic modification involving ELF6 (a H3K4 demethylases) (Jeong *et al.* 2009), as well as chromatin silencing complex EMF1c during floral induction (He 2015). The NF-Y transcription factor contributes to regulating flowering through H3K27me3 demethylation of the *SOC1* gene (Hou *et al.* 2014). Additionally, GA reduction induced by GA-biosynthesis inhibitors affect global DNA methylation levels in the GA pathway, thereby influencing floral induction (Meijón *et al.* 2011).

The MADS-box family genes, including the MIKC^c, Mα, Mβ, Mγ, and Mδ subclades in plants, act as transcription factors known to bind to DNA and perform multiple biological functions, such as floral induction and development, seed development, and fruit ripening (Smaczniak *et al.* 2012; Chen *et al.* 2017; Zhao *et al.* 2017). New hypotheses regarding the genomic origins, biological conservation, and divergence of *MADS-box* gene family members have been proposed, which are associated with multiple functions, such as regulators of floral development (*APETALA3* and *PI*), flowering time (*FLC*), and root development (*AGL17*) (Zhao *et al.* 2017). Multiple *MADS-box* genes, including the floral repressors *AGL15* and *AGL18* together with *SVP*, play negative roles in floral induction by directly binding to the *FT* promoter (Fernandez *et al.* 2014). SWP73B, a member of the SWITCH/SUCROSE NONFERMENTING chromatin remodeling complex can bind to the promoter regions of multiple *MADS-box* genes, such as *AGL24*, *SOC1*, and *AP1* to regulate flowering in *Arabidopsis thaliana* (Sacharowski *et al.* 2015). The *SOC1-like* genes *AGL42*, *AGL71*, and *AGL72* can promote flowering in the shoot apical and axillary meristems through a gibberellin-dependent pathway (Dorca-Fornell *et al.* 2011). Reduced H3K27 trimethylation at the *FLC* gene, caused by downregulation CUL4 activity, regulates flowering in the autonomous pathway (Pazhouhandeh *et al.* 2011). Class II TCP transcription factors (TFs) integrate into the FT-FD complex to control floral initiation by directly binding to the promoter of *APETALA1* (*AP1*) gene (Li *et al.* 2019).

In this study, we investigated whether there are any epigenetic changes in axillary buds of profusely flowering QA and non-flowering FA apple varieties, and whether the DNA methylation changes contribute to the expression patterns of genes involved in apple floral induction and development. We constructed whole-genome bisulfite sequencing (BS) libraries from QA and FA buds to characterize whole-genome cytosine methylation profiles. Additionally, we combined RNA sequencing data from QA and FA buds to identify gene expression patterns, as well as their correlations with methylation states, which contributes to a better understanding of epigenetic regulation mechanisms underlying floral induction and formation in apple.

2. Materials and methods

2.1. Plant materials and sample preparation

The 12-year-old QA and FA apple trees were growing in the apple orchard in Fufeng County, Baoji City, Shaanxi, China. The axillary bud with profusely flowering QA and no flowering FA were collected from 18 trees on July 2nd, 2018, respectively (Fig. 1-A and C), and then immediately frozen in liquid nitrogen. The axillary bud samples for both QA and FA were future used for RNA sequencing and whole-genome BS library construction, as well as qRT-PCR to verify gene expression with three biological replicates.

2.2. Morphological and phenotypic analysis of the QA and FA axillary buds

We used an electronic balance and a digital-display Vernier caliper to evaluate the size including length and width, and fresh weight of the axillary buds for both QA and FA (Fig. 1-C and D). Additionally, ~360 axillary buds from 12 annual apple shoots with similar length in QA and FA, respectively, were used for calculating flowering (April 10th, 2019) and germination rates (March 10th, 2019) with the previously described method (Yang *et al.* 2016; Xing *et al.* 2019a), with 12 biological replicates (Fig. 1-A and B). Longitudinal structural sections of QA and FA axillary buds were observed with paraffin section as previously described (Xing *et al.* 2019a).

2.3. Measurement of hormones contents

About 0.5 g (fresh weight) from axillary buds of QA and FA samples were used for hormones (i.e., IAA, CTK, ABA and GA) extracting with previously described method (Dobrev and Vankova 2012). And then we used a high-performance liquid chromatography system (Waters 2498 UV-Visible detector, USA) for detecting and analysis the hormones levels with as previously described method (Djilianov *et al.* 2013), with three

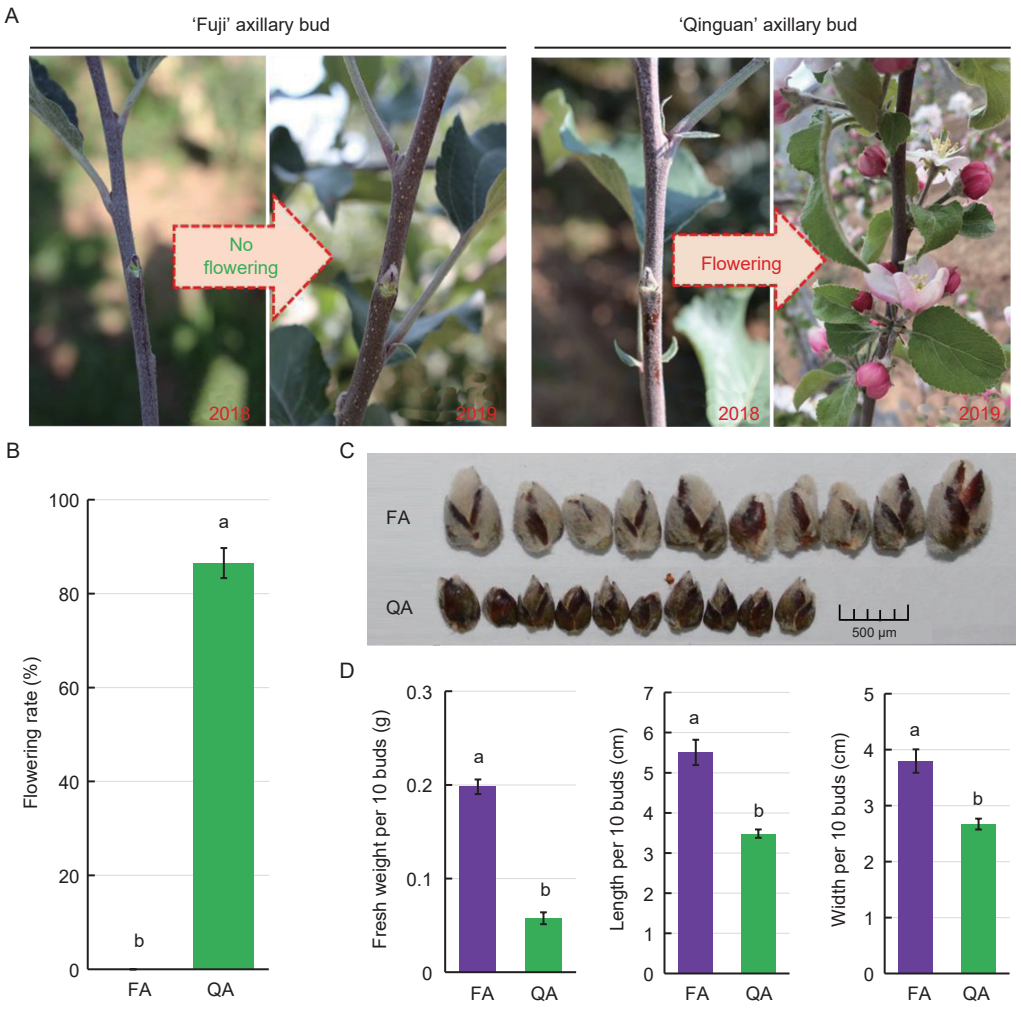


Fig. 1 Phenotypic characteristics of axillary buds in 'Fuji' (FA) and 'Qinguan' (QA). A, flowering phenotype: FA axillary buds did not flower, whereas QA axillary buds flowered on April 15, 2019. B, flowering rate. C, morphological characteristics. D, fresh weight, length and width. Data are presented as the mean±standard error (n=10). The letters a and b indicate significant differences (P<0.05) and ns indicates a nonsignificant difference (P>0.05).

biological replicates.

2.4. Bisulfite sequencing library construction, sequencing, and data analysis

We used a modified CTAB DNA extraction method for BS libraries construction from the QA and FA axillary buds (Abdel-Latif and Osman 2017). Briefly, ~5.2 μg genomic DNA was fragmented to generate 200–300 bp fragments, and then underwent an end-repair and adenylation step for sequencing with the Illumina HiSeq 2500 platform (90 cycles) by Novogene (Beijing, China) (Krueger and Andrews 2011; Feng *et al.* 2014). The clean reads by removing the adapters and low-quality reads from the raw data for both QA and FA were mapped to a high-quality de novo assembly of the apple genome (Daccord *et al.* 2017). The DNA methylation levels of the QA and FA axillary buds were analyzed by a Python script (P<0.0025) (Xing *et al.* 2019a). The raw methylation level (ML) of each cytosine site was calculated with the formula: ML (C)=Reads (mC)/Reads (mC+umC), the calculated ML was then corrected as follows, according to a previous study: ML_corrected=(ML−r)/(1−r), where r represents the bisulfite non-conversion ratio (Xing *et al.* 2019a).

2.5. Analysis of differentially methylated regions (DMRs)

The DMRs between the QA and FA were analyzed by the DSS software (Park and Wu 2016). Briefly, the DMR distribution in different gene regions involved in the gene-body region, from the transcription start site (TSS) to the transcription termination site (TTS), or the promoter region (2-kb upstream from the TSS) were analyzed with previously described method (Wu *et al.* 2015). And we used Fisher's exact test for calculating methylation levels between QA and FA with methylKit, with P-values. The identified DMRs based on the following four criteria: 1) at least three methylated cytosines in all the contexts; 2) more than 10× coverage; 3) bases (>99.9th percentile coverage) were removed to minimize errors; and 4) q-values<0.01.

2.6. RNA sequencing and identification of differentially expressed genes (DEGs)

Six QA and FA axillary buds with three biological replicates

were used for constructing RNA-seq libraries, and then sequenced with the Illumina HiSeq 2500 system by Novogene (Beijing, China) (Mortazavi *et al.* 2008). Through eliminating adapter sequences, mismatches, and low-quality reads, the clean reads were mapped to the *Malus*×*domestica* reference genome (Daccord *et al.* 2017) using the SOAP aligner/SOAP2 software (http://soap.genomi cs.org.cn/soapaligner.html) (Li *et al.* 2009). The gene expression levels were calculated according to the fragments per kilobase of transcript per million mapped reads (FPKM) values. The DEGs with FPKM were identified according to two criteria: 1) $\log_2$(fold change)>0; 2) *padj*<0.05 (Anders and Huber 2010). The Pearson correlation between the RNA-seq data and DNA methylation levels in each QA and FA axillary buds were analyzed by previously described method (Sánchez-Taltavull *et al.* 2016).

2.7. GO and KEGG functional enrichment analyses of DEGs and DMRs

Significantly enriched gene ontology (GO) terms for both DEGs and DMR-associated genes between the QA and FA axillary buds were identified (P<0.05) (http://www.geneontology.org/) (Du *et al.* 2010). Additionally, the significantly enriched KEGG pathways involved in DEGs and DMRs between QA and FA were also identified (P<0.05) (http://fttp.genome.jp/pub/kegg/pathway/) (Kanehisa *et al.* 2016).

2.8. Identification of the related genes expression levels by qRT-PCR

We used a qRT-PCR assay to identify the relative gene expression levels including DEGs and DMR-associated genes between the QA and FA with three biological replicates as previously described method (Xing *et al*. 2019b). Additionally, the information of primers used in this study are listed in Appendix A.

2.9. Statistical analysis

Data were analyzed with DPS (v7.0) (Zhejiang University, Hangzhou, China). Significant differences between QA and FA were determined by *t*-test at P<0.05. The different lowercase letters (a, b, or c) were used for indicating significant differences.

3. Results

3.1. Phenotypes characteristics of FA and QA axillary buds and their flowering ability

FA axillary buds did not flower in the next year (April 15th, 2019), but QA axillary buds could flower at the same time with a ~86% flowering rate (Fig. 1-A and B). Additionally, there were significant differences in morphological characteristics between QA and FA (Fig. 1-C), and the fresh weight, length and width of FA were significantly larger than those of QA axillary buds (Fig. 1-D). Detailed micrographs of longitudinal structural sections of QA and FA in Appendix B.

3.2. Genome-wide examination of cytosine methylation in QA and FA axillary bud

About 118.36 and 120.35 million raw reads of two BS libraries for FA and QA were generated by the Illumina HiSeq 2000 platform, respectively (yielding ~35.51 and ~36.11 Gb of data for FA and QA) (Appendix C). Additionally, 114,420,604 and 118,150,703 clean reads for FA and QA were produced, respectively, as well as 62,656,722 (54.76%) for FA and 73,170,730 (61.93%) for QA clean reads were uniquely mapped to the *Malus*×*domestica* reference genome (Daccord *et al.* 2017) (Appendix D). The detailed information of gene coverage for FA (76.4, 63.12 and 20.42%) and QA (77.11, 63.62 and 18.78%) involved in CG, CHG and CHH contexts, respectively, is indicated in Appendix E.

The circus plots showed that the whole chromosome-wide distribution of DNA methylation involved in the density of 5mC in the CG, CHG, and CHH contexts, the density of TEs, the genes and RNAs density of each chromosome for QA and FA (Fig. 2-A and B; Appendix F), indicating that there were significant differences in these indicators among various chromosomal positions. Additionally, there were similar proportions of methylation levels in CG, CHG and CHH contexts for FA (i.e., 19.35, 62.96 and 17.68% for CG, CHG and CHH, respectively) and QA (19.64, 62.49 and 17.86% for CG, CHG and CHH, respectively) (Fig. 2-C). Detailed information on the percentage of methylated cytosine in the CG, CHG, and CHH contexts across each chromosome is shown in Fig. 2-D, indicating that the percentage of CG context was significantly higher than that of CHG and CHH in both FA and QA. However, the mean methylation levels involved in CG, CHG and CHH contexts were significantly higher in QA than in FA (Fig. 2-E). Bisulfite sequencing data on the mean depth and proportion of covered bases in each chromosome for the QA and FA are provided in Appendix G. The methylation densities and levels in all contexts in QA and FA were in Appendix H.

3.3. Distribution of DNA methylation in genic regions

A heatmap analysis showed that DNA methylation levels differed significantly among different gene features, including promoters, exons, intron, and repeat regions (Appendix A). The DNA methylation levels in the CG, CHG and CHH contexts for both FA and QA were highest in the repeat regions, followed by promoter, intron and exon regions (Appendices A and B). Additionally, the DNA methylation levels in all contexts were higher in the 2-kb upstream and downstream regions of the gene-bodies than in the gene bodies themselves (Appendix C).

Circos plots showed that there were significant differences in the CG, CHG, and CHH contexts in the whole chromosome-wide distribution of DNA methylation levels between FA and QA (Fig. 3-A). DNA methylation levels in the CG, CHG, and CHH contexts were similar between FA and QA across all different gene regions (i.e., promoters, exons, introns, and other regions) (Fig. 3-B), as well as in gene bodies and the 2-kb upstream and downstream regions of the gene bodies (Fig. 3-B). Specifically, the DNA methylation levels in exon regions for the CG and CHG contexts were significantly higher in QA than in FA (Fig. 3-B), but the DNA methylation levels in promoter regions for the CHH context, in intron regions for

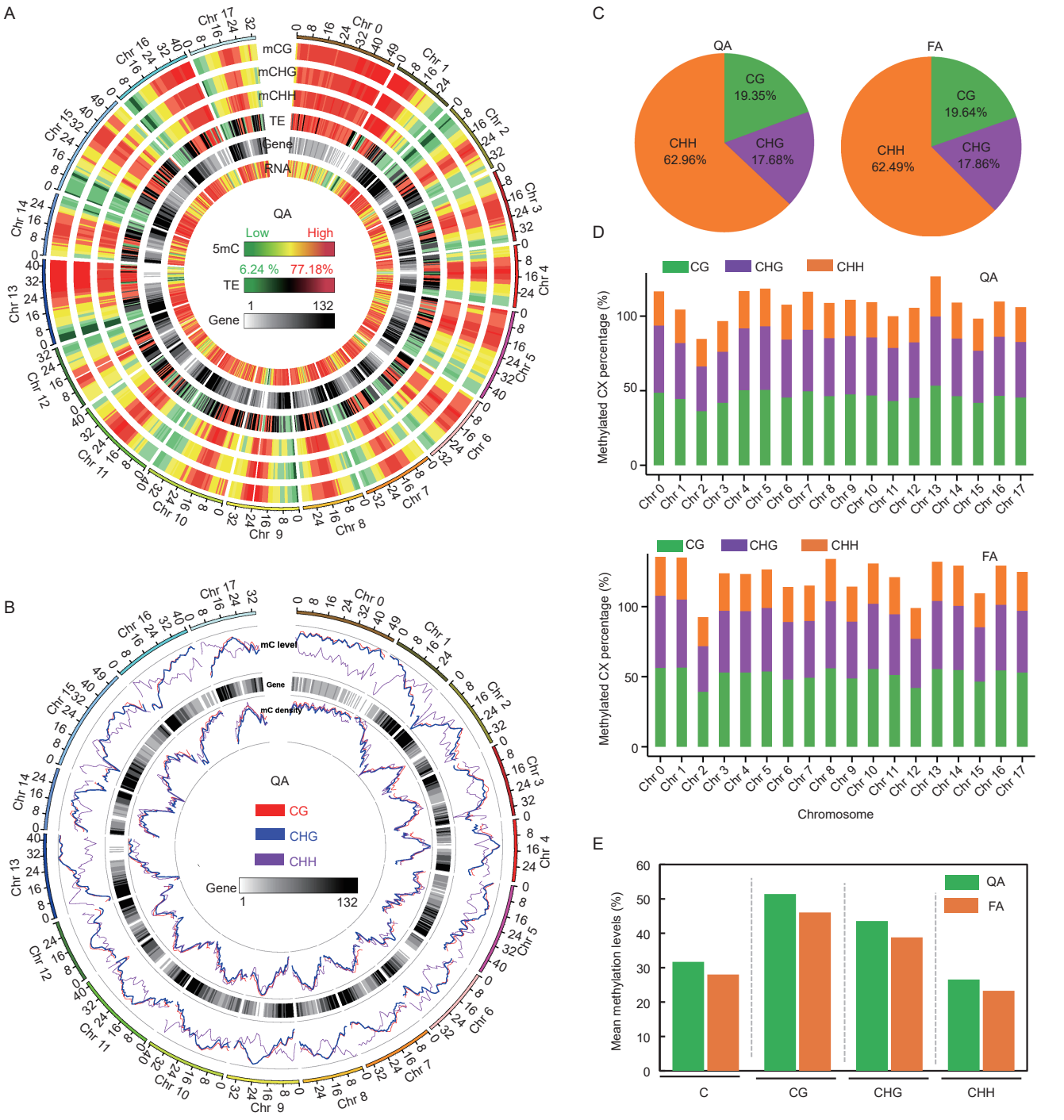


Fig. 2 Epigenomic profiling of axillary buds in 'Qinguan' (QA) and 'Fuji' (FA). A, Circos plots of chromosomes in the QA. Track order: 5mC density in CG, CHG, and CHH contexts; transcription end sites (TEs) density; and gene and RNA density of each chromosome. B, 5mC density plots in CG, CHG, and CHH contexts in gene bodies across each chromosome in QA. C, relative proportions of methylated cytosines (mCs) in CG, CHG, and CHH contexts in QA and FA. D, percentage of methylated CX in the CG, CHG, and CHH contexts on each chromosome in QA and FA. E, mean methylation levels in CG, CHG, and CHH contexts in QA and FA. The "C" on the *x*-axis indicates total cytosines.

CHG and CHH contexts, and in repeat regions for the CHH context showed the opposite results (Fig. 3-B). Additionally, for the CHH context in gene bodies and the 2-kb upstream and downstream regions of the gene bodies, the DNA methylation levels in QA were significantly lower than those in FA (Fig. 3-C), but for the CG context in gene body regions, the opposite result was observed between QA and FA (Fig. 3-C).

3.4. Identification of DMRs between axillary bud with profusely flowering QA and no flowering FA, and functional annotation analysis

Circos plots showed that the whole-genome chromosome-wide distribution of DMRs (FDR<0.05) for both hypermethylated and hypomethylated regions in the CG, CHG, and CHH contexts between FA and QA (Fig. 4-A;

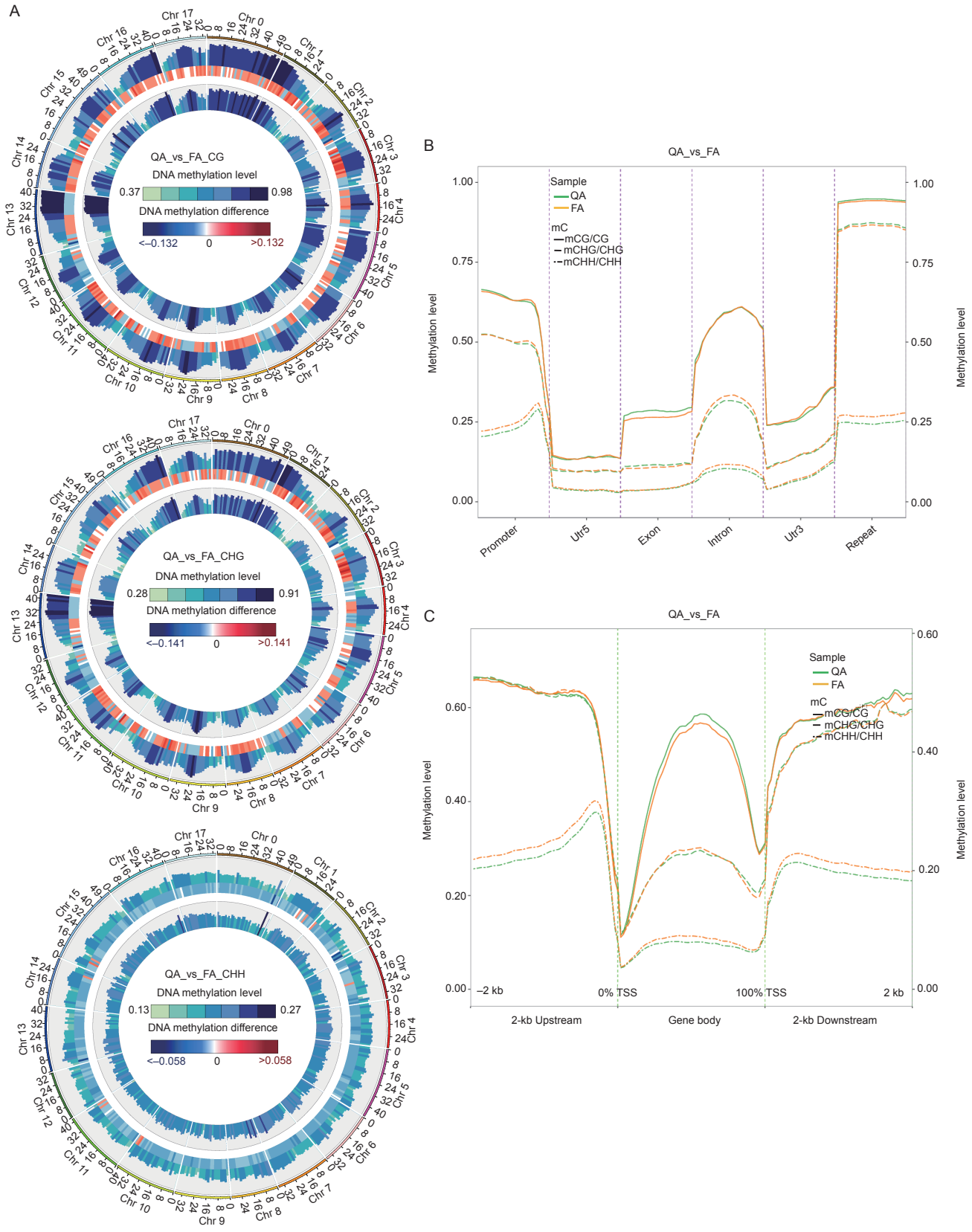


Fig. 3 Comparative analysis of DNA methylation levels in various genomic regions between 'Qinguan' (QA) and 'Fuji' (FA) axillary buds. A, Circos plots comparing DNA methylation levels involved in the CG, CHG and CHH contexts between QA and FA. B, comparison of the distribution of DNA methylation levels involved in the CG, CHG and CHH contexts in various genomic regions between QA and FA. C, comparison of the methylation levels involved in the CG, CHG and CHH contexts in gene bodies and their 2-kb upstream and downstream regions between QA and FA. In Fig. 3-C, the left *Y*-axis represents the methylation levels of CG and CHG types, while the right *Y*-axis represents the methylation level of the CHH type.

Appendix G). Venn diagrams show unique or common DMRs in genes (QA_vs_FA_DMRs_genes) and in promoter regions (QA_vs_FA_DMRs_promoter_genes) between FA and QA in the CG, CHG, and CHH contexts (Fig. 4-B). Specifically, the QA_vs_FA comparison group contained 2,820, 1,426, and 1,808 DMR_genes (Fig. 4-B) as well as 2,853, 2,462, and 2,547 DMR_promoter_genes in the CG, CHH, and CHG contexts, respectively (Fig. 4-B). Additionally, the DMR methylation levels in the CG and CHG contexts of the DMRs were significantly higher in QA than in FA, but those in the CHH context had the opposite result between FA and QA (Fig. 4-C). A heatmap also showed the visual information of the DMRs and their DNA methylation levels in all three contexts (FDR<0.05) between FA and QA (Fig. 4-D). The numbers of the hypermethylated or hypomethylated DMRs in all contexts also had a significant differences among different genic regions (i.e., the promoter, TSS, TTS, exon, repeat, and other regions) (Fig. 4-E). For example, the numbers of DMRs (i.e., hypermethylated or hypomethylated) in TSS, TTS, 5´UTR, and 3´UTR regions were significantly fewer than those in other regions including promoter, exon, and repeat regions (Fig. 4-E). Additionally, the numbers of hypermethylated DMRs in the CG and CHG contexts in repeat regions were significantly greater than those of hypomethylated DMRs between FA and QA, but for the CHH context, the opposite result was observed (Fig. 4-E).

To know the function of the DMR_genes and DMR_promoter_genes, the most enriched GO terms were identified for both hypermethylated and hypomethylated genes in QA compared with FA, in CG, CHG and CHH contexts (Appendices K and L). For example, the most enriched GO terms included metabolic process, cellular process, biological regulation for QA_vs_FA_hypermethylated genes in the CG context (Appendix K). For DMR_promoter_genes, the most enriched GO terms for QA_vs_FA_hypermethylated genes in the CG context were: metabolic process, cellular process, and biological regulation (biological process), cell, cell part, and organelle (cellular component), and binding, catalytic activity, and transporter activity (molecular function) (Appendix L). KEGG pathway analysis also revealed some significantly enriched pathways associated with DMR_genes and DMR_promoter_genes for the QA_vs_FA comparison group (Appendices M and N), including metabolic pathways and biosynthesis of secondary metabolites for hyper/hypo-DMR_genes in the CG context (Appendix M). Additionally, information regarding the significantly enriched pathways for the hyper/hypo-DMR_promoter_genes in the CG, CHG, and CHH contexts is provided in Appendix N.

3.5. Transcriptome profiling and functional analysis of DEGs between axillary bud with profusely flowering QA and no flowering FA apple

Hierarchical clustering heatmaps showed the DEGs in the QA_vs_FA comparison group, including 19,656 (9,543 downregulated and 10,113 upregulated) with $\log_2$(fold change)>0 and *padj*<0.05 (Fig. 5-A and B). GO functional analysis revealed the most enriched terms for the DEGs in QA and FA, involving in biological process, i.e., oxoacid metabolic process, organic acid metabolic process, and catabolic process (upregulated genes); signaling, signal transduction, and single organism process (downregulated genes), cellular component, i.e., membrane protein complex, thylakoid, and thylakoid part (upregulated genes); cell periphery, cell cortex, and plasma membrane part (downregulated genes) and molecular function, i.e., peptidase activity, endopeptidase activity, and transferase activity (upregulated genes); calcium ion binding, ubiquitin-protein transferase activity, and calmodulin binding (downregulated genes) (Fig. 5-C). Additionally, the most enriched KEGG pathways in QA compared with FA were: plant–pathogen interaction, spliceosome, and amino sugar and nucleotide sugar metabolism (upregulated genes); and carbon metabolism, biosynthesis of amino acids, and protein processing in endoplasmic reticulum (downregulated genes) (Fig. 5-D). Additionally, the gene expression distribution and Pearson correlation among QA and FA samples are provided in Appendix O. Details regarding the RNA-sequencing data for both QA and FA are provided in Appendices P and Q.

3.6. Association between DNA methylation and transcript abundance

The gene expression levels were divided into the following four quartiles based on their FPKM values: non-expressed (FPKM<1), low expression level (1≤FPKM<25%), medium expression level (25%≤FPKM<75%), and high expression level (FPKM≥75%) (Fig. 6-A). We found that the lowly expressed genes had high methylation levels, highly expressed genes had low methylation levels in the gene-body for CG, CHG and CHH contexts, and upstream of the TSS and downstream of the TTS regions for CG and CHG contexts for both QA and FA (Fig. 6-A). However, for CHH context, the most highly expression genes had the high methylation levels in upstream of the TSS and downstream of the TTS regions (promoter regions) in both QA and FA (Fig. 6-A).

To know the correlation between the gene methylation and expression levels, the methylated genes were divided into the following five quintiles based on the promoter and gene-body methylation levels: group 1 (methyl_level<20%), group 2 (20%≤methyl_level<40%), group 3 (40%≤methyl_level<60%), group 4 (60%≤methyl_level<80%), and group 5 (methyl_level≥80%) (Fig. 6-B). We also found that methylation levels had a negative regulatory relationship with gene expression levels involved in the CG, CHG, and CHH contexts in the gene-body region, and CG and CHG contexts in upstream of the TSS and downstream of the TTS regions (promoter regions), but they had a positive regulatory relationship when the methylation in CHH context happened in promoter regions (upstream of the TSS and downstream of the TTS regions) for both QA and FA (Fig. 6-B). Additionally, the detailed information about the relationship between methylation difference and gene expression (FPKM) involved in CG, CHG and CHH contexts for both hypermethylated and hypomethylated DMRs in different regions (i.e., gene-body and promoter) in QA compared with FA is presented in Fig. 7-A–C.

3.7. Huge differences in transcription of MIKC^c-type *MADS-box* genes by changing DNA methylation, contributed to contrasting flowering behaviors

We identified 132 *MADS-box* family genes in apple that belong to five subgroups (i.e., MIKC^c, Mβ, Mα and Mδ) (Fig. 8-A; Appendix R). Among the differentially expressed *MADS-box* family genes were mainly belong to MIKC^c subgroup between QA and FA, but no differentially

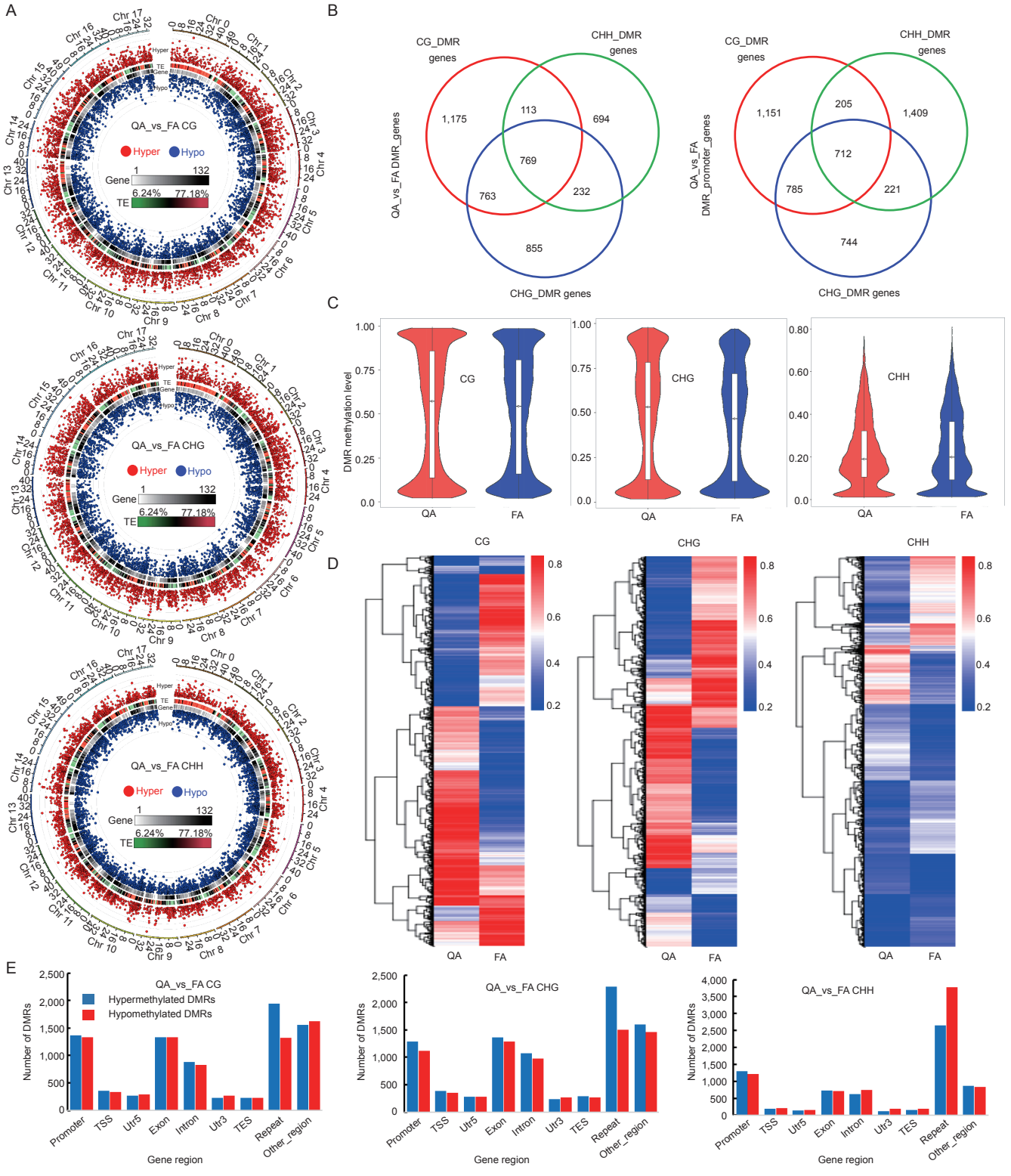


Fig. 4 Differentially methylated regions (DMRs) between 'Qinguan' (QA) and 'Fuji' (FA) axillary buds. A, Circos plots comparing the DMRs between QA and FA. B, Venn diagram analysis of genes with DMRs in the gene body regions, as well as in the promoter regions between QA and FA. C, methylation levels of the DMRs between QA and FA. D, heat maps of DMRs in the CG, CHG, and CHH contexts between QA and FA. E, number of DMRs associated with the hyper-/hypomethylated in various genomic regions.

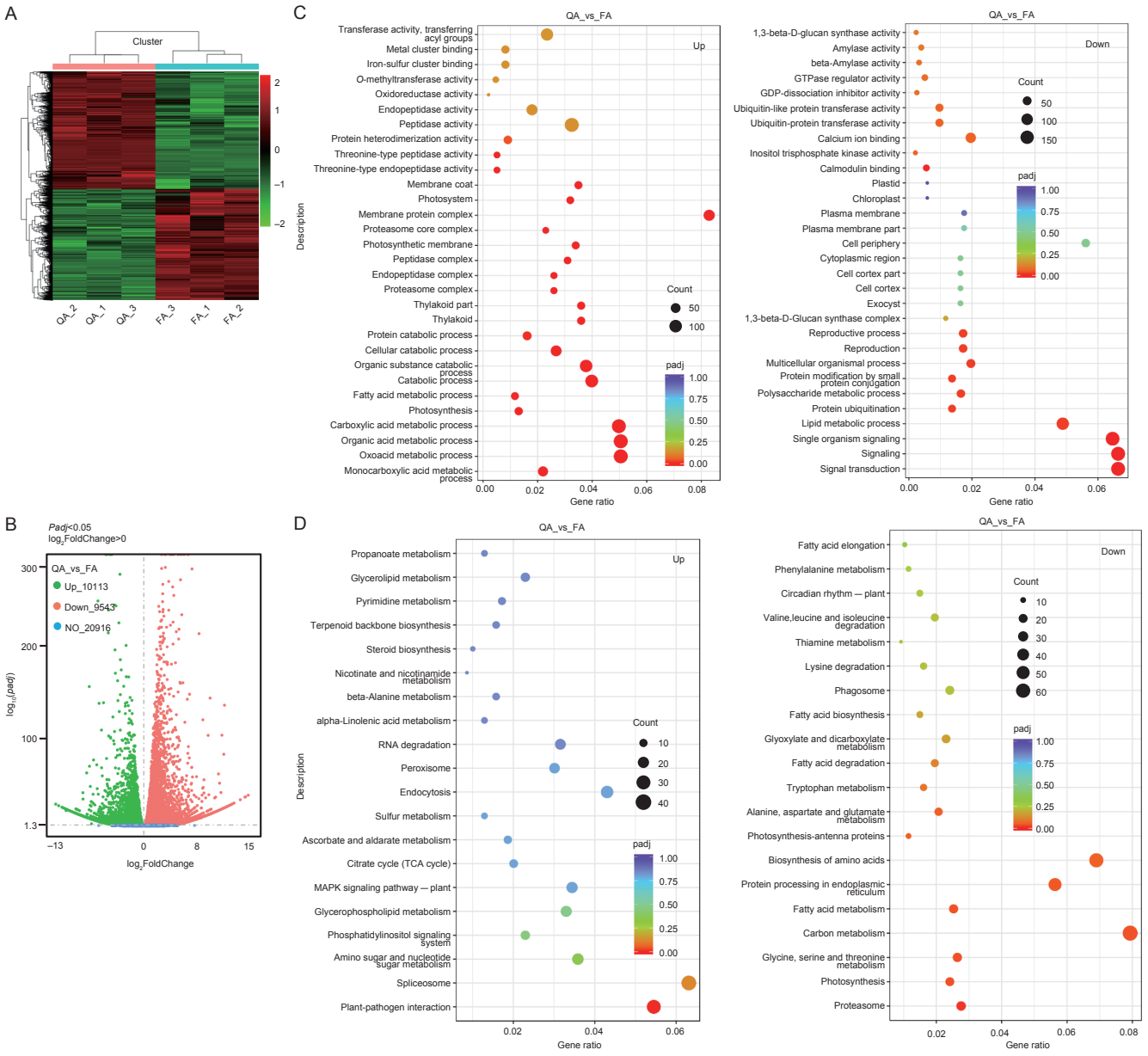


Fig. 5 Differentially expressed genes (DEGs) between 'Qinguan' (QA) and 'Fuji' (FA) axillary buds and their functional analysis. A, heat maps of DEGs. B, Volcano plot of the DEGs. C, significantly enriched GO function terms of the DEGs. D, significantly enriched KEGG pathways of DEGs between QA and FA.

expressed *MADS-box* genes were found in the other two subgroups (Mα and Mδ) (Fig. 8-A). Eleven differentially expressed *MADS-box* genes that belong to cluster I (i.e., *AGL16*_MD08G1206400; *AGL18*_MD00G1106300; *SEP1*_MD06G1204100/MD09G1009100; *SEP4*_MD13G1059300) were significantly lower expression in axillary bud with profusely flowering QA than FA, but other 17 differently expressed *MADS-box* genes belong to cluster II (i.e., six *AGL24*, three *AGL80*, *AGL6*, *AGL79* and *AGL24*) had an opposite result (Fig. 8-B; Appendix A). Specially, flowering key genes (*SOC1*_MD07G1123600 and *AP1*_MD06G1204400), as well asidentify genes (*AG*_MD10G1271000 and *AP3*_MD02G1136500) belonged to cluster II that showed higher expression levels in axillary bud with profusely flowering QA. However, the key negative regulation gene in floral induction (*SVP*_MD01G1038600/MD15G1384600) belong to cluster I were significantly lowerly expressed in axillary bud with profusely flowering in QA (Fig. 8-B; Appendix S). Additionally, the methylation levels of thirteen *MADS-box* family genes (i.e., *AGL21*_intron_CHG, *AGL21*_promoter_CHH and *AGL12*_intron_CHH and *AGL62*_exon_CHG) in different gene regions were significantly higher expression in axillary bud with profusely flowering QA than FA (Fig. 8-C), which were contributed to down-regulation of these genes in axillary bud of QA than in FA. However, other eleven DMRs (i.e., *AGL30*_exon_CG, *AGL42*_promoter_CG, and *AGL42*_promoter_CHG) had an opposite methylation

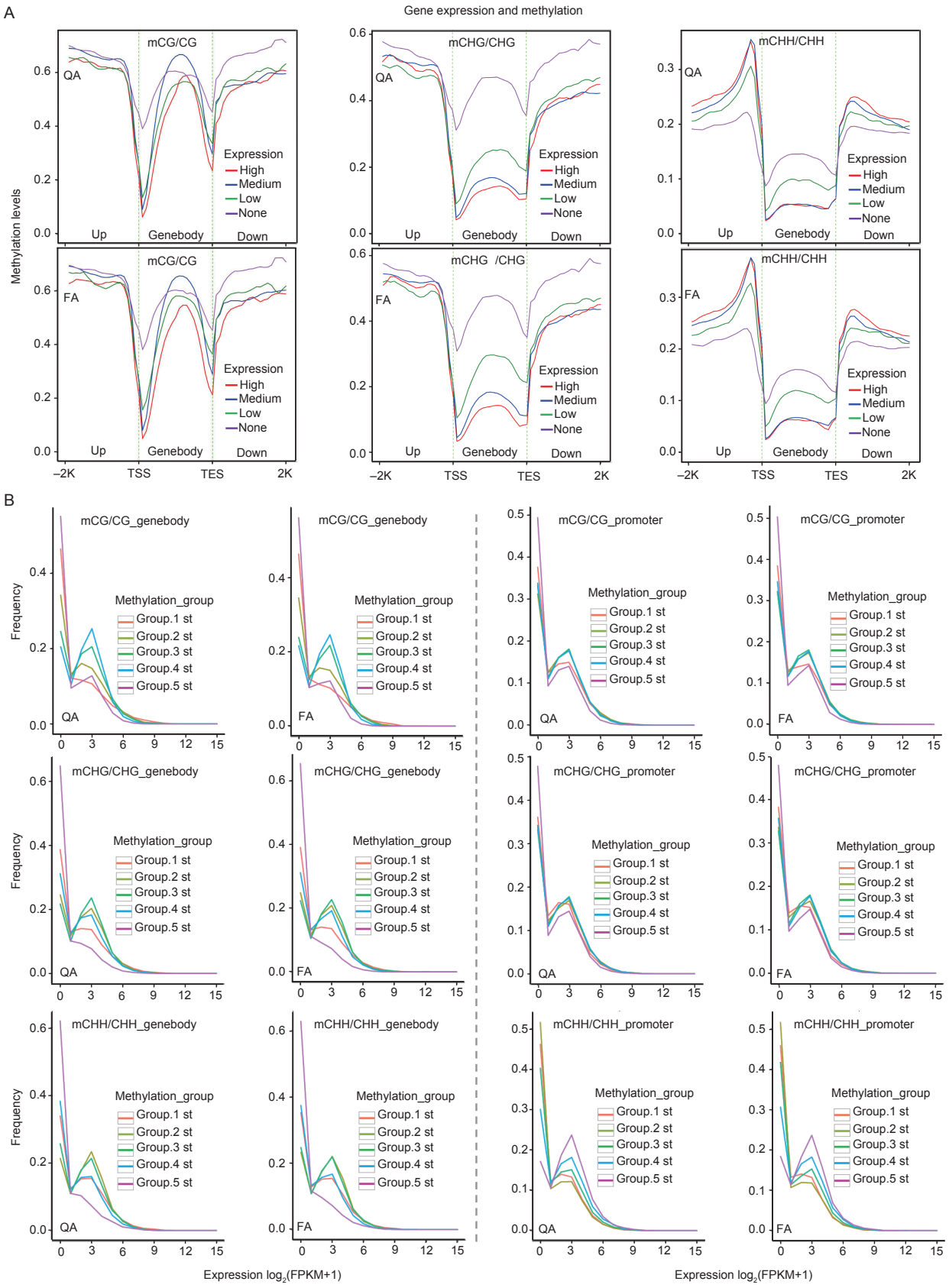


Fig. 6 Correlation between DNA methylation and gene expression. A, distribution of methylation levels in various genomic regions, from low to high expression levels as follows: non-expressed (none; FPKM value<1); low expression level (1≤FPKM<25%); medium expression level (25%≤FPKM<75%); and high expression level (FPKM≥75%). B, expression profiles of methylated genes in QA and FA. Methylated genes from lowest to highest as follows based on methylation levels: group 1 (methylation<20%); group 2 (20%≤methylation<40%); group 3 (40%≤methylation<60%); group 4 (60%≤methylation<80%); and group 5 (methylation≥80%).

pattern between axillary buds of QA and FA apple, which may contribute to the regulation of these MADS-box genes expression involved in promoting flowering in QA axillary bud (Fig. 8-C). Similarly, IGV snapshots presented the representative DMRs that were hypermethylation or demethylation between the axillary buds of QA and FA, including *AGL80*_MD00G1098000_CHH, *AGL42*_MD01G1103300_CG, and *AGL42*_MD00g1004500_CG in the promoter, and *AGL79*_MD17G1001300_CHH in the intron, and *AGL30*_MD13G1070300_CG in the exon (Fig. 8-D). Additionally, differently expression of *MADS-box* genes formed complex gene interaction regulatory networks including floral promoter (i.e., *SOC1* and *AGL42*), floral organ identify (i.e., *AG* and *AP3*), and floral repressor (i.e., *SVP* and *AGL18*), contribute to regulation of flowering in axillary buds of QA (Fig. 9).

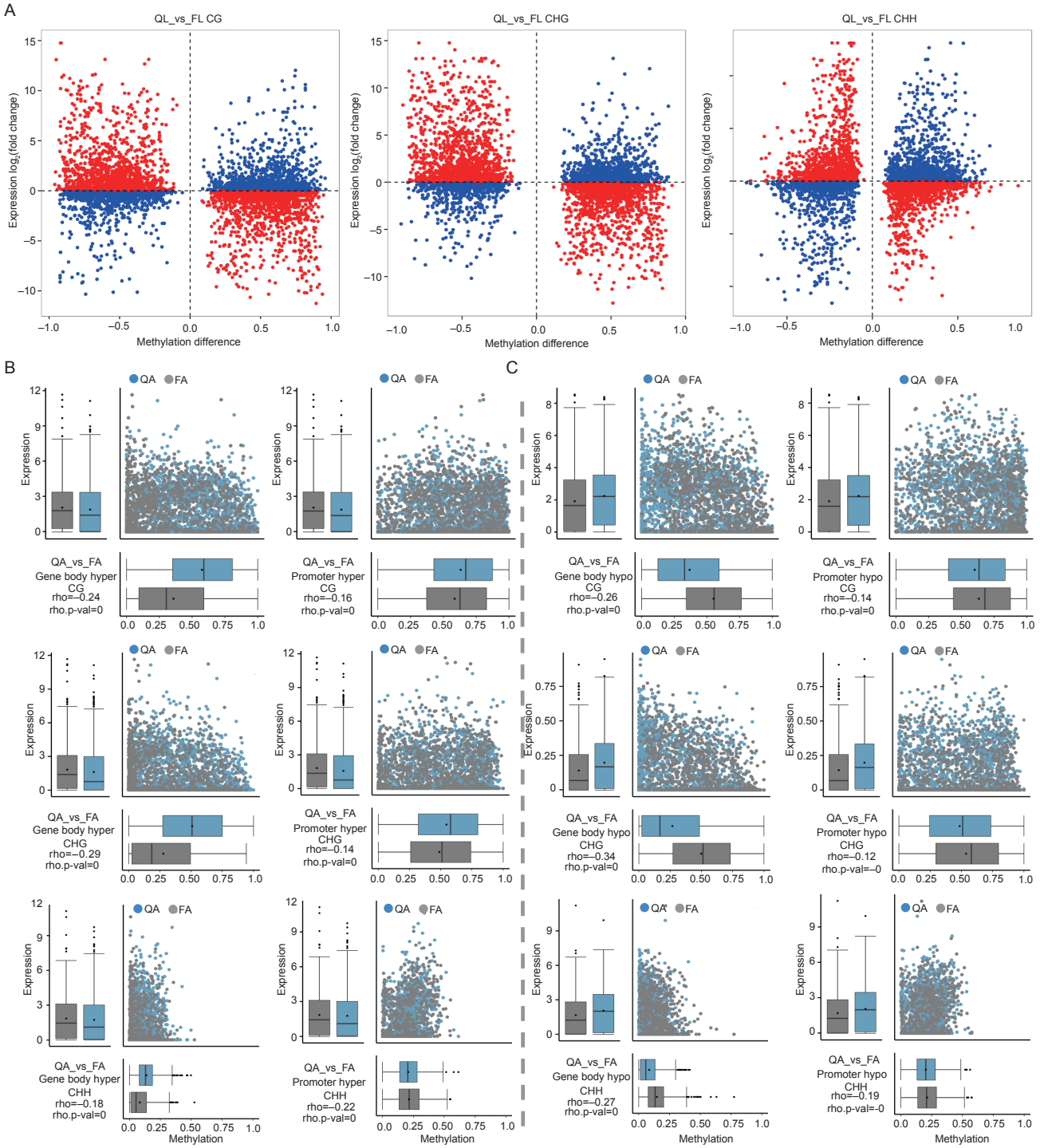


Fig. 7 Correlation analysis of gene expression and methylation difference. A, scatter diagram of correlation analysis. B, gene expression and hypermethylation DMR genes in gene body and promoter regions. C, gene expression and hypomethylation DMR genes in gene body and promoter regions.

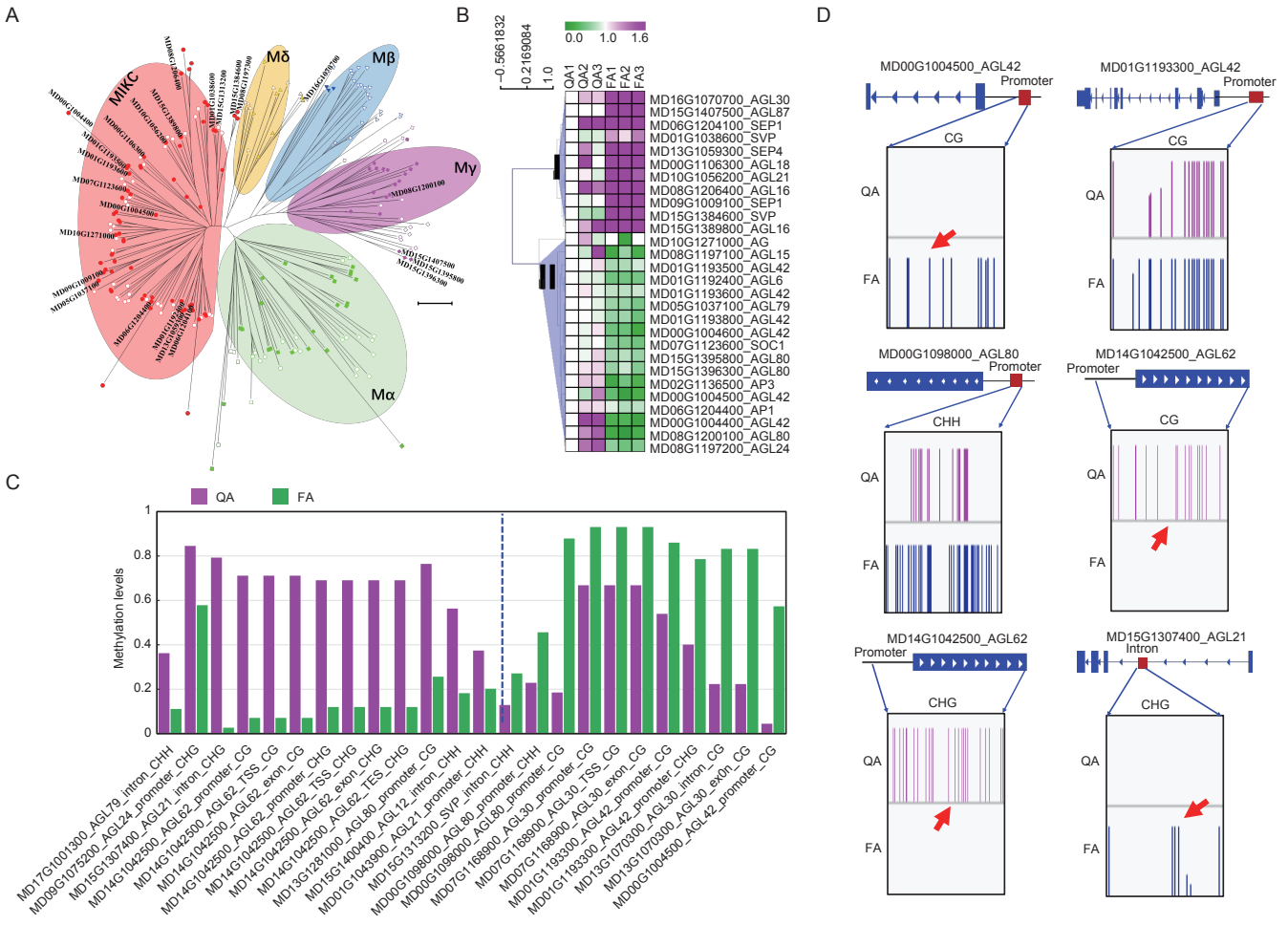


Fig. 8 Methylation and expression levels of MADS-box family genes. A, phylogenetic analysis of the differentially expressed genes (DEGs) and differentially methylated regions (DMRs) in MADS-box family genes. B, heat maps of the differently expression of MADS-box family genes. C, methylation levels of DMRs in MADS-box family genes. D, integrative genomics viewer snapshots of the representative DMRs in MADS-box family genes between 'Qinguan' (QA) and 'Fuji' (FA).

3.8. DEGs in multiple flowering pathways between axillary buds of QA and FA apple by changing DNA methylation, contributed to contrasting flowering behaviors

We identified these DEGs and DMRs in multiple flowering regulatory pathways between axillary buds of QA and FA apple (Fig. 10; Appendices T and U). Firstly, these genes involved in key floral meristem identify (i.e., *LFY*, *AP1*, *SOC1* and *FT*) were expressed significantly higher in axillary buds of QA than in FA (Fig. 10-A). In the age pathway, eleven *SPL* genes that can directly up-regulate *LFY* and *SOC1* showed significantly higher expression in QA axillary buds than in FA, but there was an opposite result for two *AP2-like* and one *TOE* genes involved in negative regulation of *SOC1* expression (Fig. 10-A). In the photoperiodic pathway centered on the *CO* gene, seven *COL* and eleven BBX genes were expressed significantly lower in QA axillary buds than in FA, and the upstream regulators of the *CO* gene, such as five *COPs*, three *SPAs*, *PHYA*, *CRY1* and *CRY2* showed a similar result (Fig. 10-A). Another upstream regulator of *CO* gene involved in the circadian clock pathway, including *FKF1*, two *CDF2* and two *CDF3*, three *PRR* and *TOC1* also had a similar result (Fig. 10-A). However, two *NF-YA*, four *NF-YB* and four *NF-YC* that can interact with the *CO* gene were expressed significantly higher in axillary buds of QA than in FA (Fig. 10-A). In the vernalization and autonomous pathway, these genes were significantly upregulated in FA compared with QA including two *MSI1*, *SWN* and *VIN3*, as well as two *FLK* and *FY* that can directly inhibit the expression of the *FLC* gene to promote flowering (Fig. 10-A). Additionally, the FAF1-like complex including *ELF5*, *EFS*, *ATX2*, three *SDG2*, two *VIP4* and *VIP5*, and the SWR1/SRCAP-like complex including *ARP5*, *ARP6*, *SEF* and *PIE1* — which can directly promote the expression of the *FLC* gene to inhibit flowering — were expressed significantly higher in FA than in QA, a pattern that contributed to promoting floral induction in QA (Fig. 10-A). Furthermore, the genes including *REF* and *SRP1* involved in histone modification were also significantly differentially expressed between axillary buds of QA and FA (Fig. 10-A), suggesting they play a key role in regulating the flowering process in QA. In the sugar pathway, two types of genes (i.e., *IDD4/5* and *SUS4*) belonging to the upstream regulators of *FT* and *SPL* genes were expressed significantly

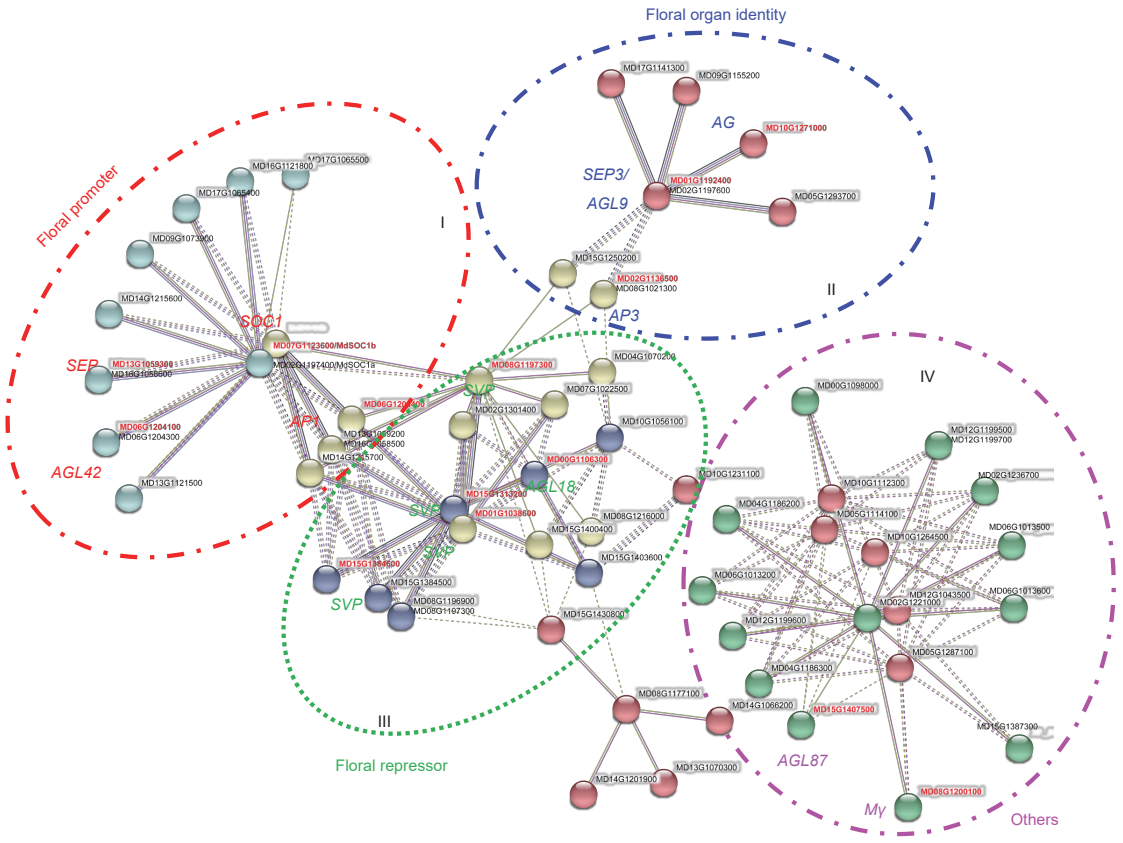


Fig. 9 Interactive network analysis of the differently expression of MADS-box family genes.

higher in axillary buds of QA than in FA (Fig. 10-A). And five *TPS14* genes showed higher expression in QA than in FA, but one *TPS2* and *TPS4*, as well as five *TPS21* genesshowed the opposite result (Fig. 10-A), indicating that *TPS* genes play multifaceted functions in flowering within the sugar pathway. In addition, two *RGA2* genes in the GA pathway showed significant differential expression between axillary buds of QA and FA, which contributed to their different flowering abilities (Fig. 10-A).

We also identified many DMRs between axillary buds of QA and FA that were involved in multiple flowering pathways (Fig. 10-B). For example, five DMRs (i.e., *LFY*_MD14G1146700_CG in the promoter, and *ELF4*_MD11G1074300_CHH in an exon) belonging to cluster I showed significantly lower methylation levels in the axillary buds of profusely flowering QA than in those of FA across flowering pathways (Fig. 10-B), but 16 DMRs (i.e., *SPL1*_MD16G1137700_CHH, and *SLP14*_MD14G1060299_CHH in the promoter; *TFL1*_MD12G1023900_CG in the promoter and *TFL2*_MD07g1081800_CG in an exon) belonging to cluster II showed the opposite result (Fig. 10-B). In the photoperiodic pathway, 21 DMRs belonging to cluster II, such as *COL4*_MD16G1148500_CG, and *CRY2*_MD16G1217800_CHG, *DOF*_MD15G126570_CG/CHG in an exon, *BBX32*_MD17G1147000_CG/CHG in an exon showed significantly higher methylation levels in QA than in FA (Fig. 10-B), but *BBX32*_MD17G1147000_CHH in the promoter and *COP9*_MD09G1015400_CG in an exon, belonging to cluster I showed the opposite result, suggesting that these DMRs in different regions may contribute to regulate genes expression levels. Similarly, six DMRs (i.e., *SPA3*_MD11G1247500_CG in an exon and *SDG2*_MD17G1091000_CHG in the promoter) belonging to cluster I showed significantly lower methylation levels in QA than in FA, and 19 DMRs (i.e., *ARP4*_MD03G1252000_CG in an exon, and *VIN3*_MD08G1199400_CG in the promoter) belonging to cluster II showed the opposite result (Fig. 2-B). In the sugar and GA pathways, five DMRs: *TPS21*_MD03G1214900_CHG in an intron, *GRA*_MD13G1022100_CG/CHG in an exon and *GRA*_MD13G1022100_CHH in the promoter, and *TPS21*_MD03G1207000_CHH in an exon, belonging to cluster I, showed significantly higher methtlation levels in FA than in QA, but those DMRs belonging to cluster II (i.e., *IDD5*_MD16G1009600_CHH in the promoter, and *GAI*_MDMD17G1260700_CHG in an exon, and *GAI*_MDMD17G1260700_CG in the promoter) showed the opposite result (Fig. 10-B).

Additionally, IGV snapshots showed these were multiple DMRs in different gene regions between QA and FA that affected gene expression, such as hypermethylation in QA compared th FA (i.e., *SPL14*_CHH, *CRY1*_CHH in the promoter, *PHYB*_CG, and *TPS21*_CHG in an exon, as well as *BBX32*_MD17G1147000 involving CG, CHH and CHG contexts in the exon region) or hypermethylation in QA compared to FA, such as *NF-YB*_MD00G1101600 involving CG, CHH and CHG contexts in the exon region (Fig. 10-C). This suggests that gene

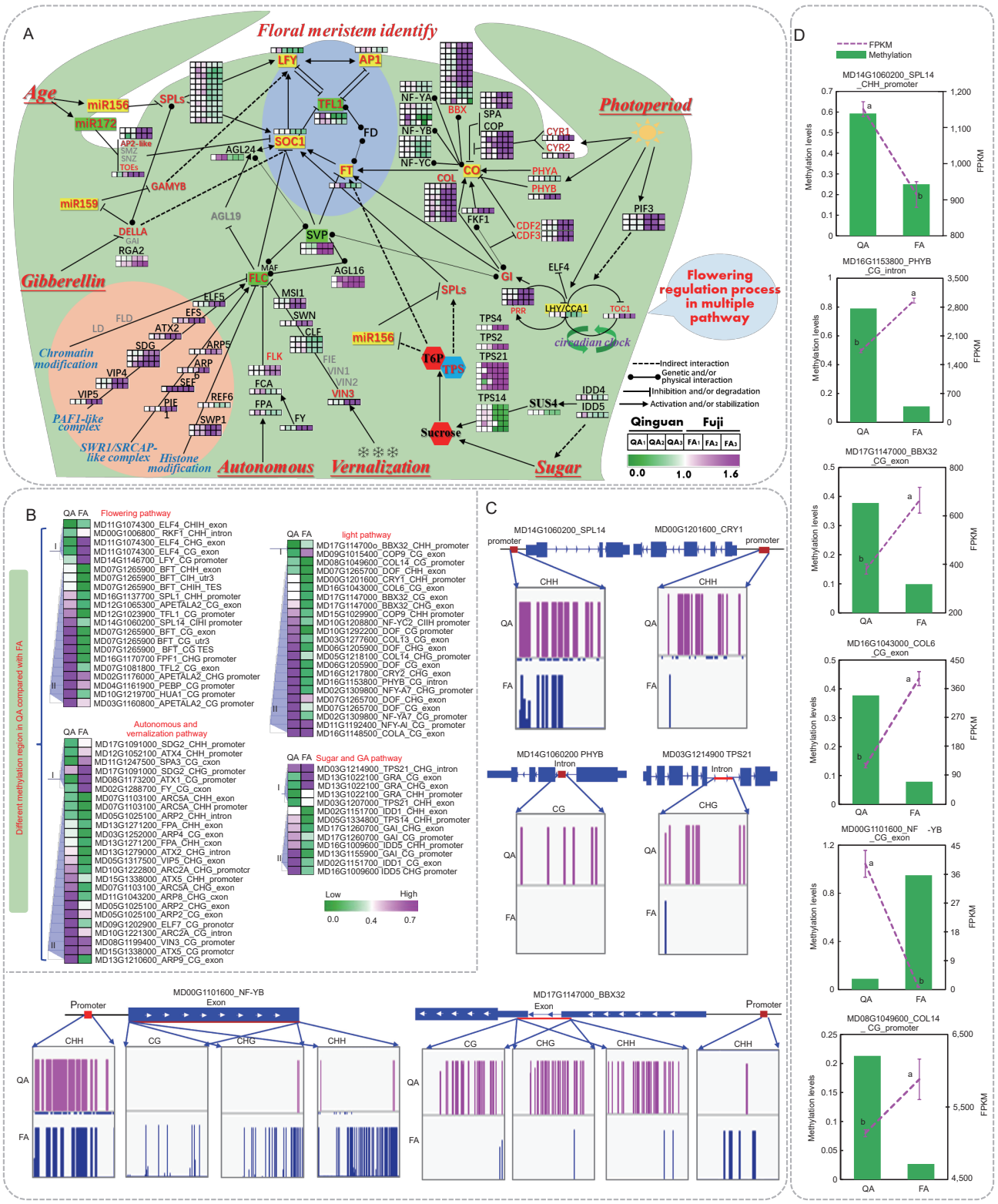


Fig. 10 The differentially methylated regions (DMRs) and differentially expressed genes (DEGs) involved in multiple flowering pathways between 'Qinguan' (QA) and 'Fuji' (FA). A, the complex flowering regulatory network involved in the DEGs between QA and FA. B, the DMRs in QA *vs*. FA. C, integrative genomics viewer snapshots of the DMRs in the representative flowering genes. D, the methylation and gene expression levels of the representative flowering genes in multiple flowering pathways. Data are presented as the mean±standard error (n=3). The letters a and b indicate significant differences and ns indicates a nonsignificant difference (P>0.05).

expression was regulated by these DMRs in different regions. We also found that these DMRs in different regions involving CG, CHH and CHG contexts were negatively correlated with gene expression levels, such as *BBX32*_CG _exon, *COL6*_

CG_exon, *NF-YB*_CG_exon, and *COL14*_CG_promoter (Fig. 10-D). In contrast, DMRs in promoter involving the CHH context were positively correlated with gene expression, such as *SPL14*_MD14G1020600_CHH in the promoter (Fig. 10-D). These results indicate that DNA methylation can positively or negatively regulate gene expression.

3.9. Effects of DEGs and DMRs in hormone synthesis pathways on axillary bud outgrowth and flowering

There were significant differences in multiple plant hormones levels between axillary buds of QA and FA (Fig. 11-A; Appendix V). The ABA and GA contents were significantly higher in QA than in FA, while there was no significant difference in IAA levels; however, the CK content showed the opposite pattern (Fig. 11-A). These differences are associated with the significantly higher rates of germination and flowering in QA than in FA (Fig. 11-A).

In addition, the expression of genes involved in ABA biosynthesis, such as *ZEP*, three *NCED1*, two *NCED4*, and two *ABA2* was significantly higher in axillary buds of FA than in QA, a similar result was observed for key GA biosynthesis genes (i.e., two *CPS1* and *KS*) in our data (Fig. 11-A). In contrast, the expression of genes involved in converting active GAs to inactive forms (i.e., *GA2OX1*, *GA2OX2*, and *GA20X8*) showed the opposite pattern (Fig. 11-A), which contributed to lower GA levels in QA than in FA. We also found that *IPT2* gene involved in CK biosynthesis and *YUCC8* involved in IAA biosynthesis were expressed significantly higher in QA than in FA, which may lead to higher levels of CK in QA than in FA (Fig. 11-A). Interestingly, genes involved in SL biosynthesis (i.e., *D27*, *MAX3*, *MAX4*, and *MAX1*) showed no significant difference in expression between QA and FA (Fig. 11-A). However, genes belonging to SL signaling, including three *D14* and two *MAX2*, were expressed significantly higher in FA than in QA (Fig. 11-A). These genes are involved in the regulation of axillary bud outgrowth and formation through targeted regulation of *BRC1*, as well as being regulated by auxin. Additionally, multiple *PIN* genes (i.e., two *PIN1*, *PIN3*, and five *PIN-like*) involved in IAA transport from axillary buds to other organs were expressed significantly higher in QA than in FA (Fig. 11-A). This may result in relatively lower IAA levels in axillary buds of QA, thereby promoting axillary bud outgrowth compared with FA.

Additionally, the *GA2OX8* gene (MD05G1341000), a key gene involved in GA biosynthesis, exhibited lower methylation (demethylation) in exon regions across the CG, CHG, and CHH contexts in QA relative to FA (Fig. 11-B). This was associated with the relatively higher of *GA2OX8* in QA, negative correlation between DNA methylation and gene transcription level. Additionally, the methylation level of *PIN1*_MD12G1095100 in the CHH context in the promoter region was also significantly higher in FA than in QA, but the expression of *PIN1* had an opposite result between FA and QA (Fig. 11-B), suggesting that DNA methylation play key roles in gene expression.

3.10. Identification of related DEGs by a qRT-PCR assay

The expression levels of these representative flowering genes (i.e., *FT*_MD12G1262000, *SOC1*_MD07G1123600, *AP1*_MD06G1204400, *SPL4*_MD17G1236000, *PHYA*_MD04G1183900) were significantly higher in QA than in FA, according to both qRT-PCR and RNA-seq data (Fig. 12-A). In contrast, COL2_MD09G1079200 showed the opposite expression pattern. Furthermore, a linear relationship was observed between the qRT-PCR and RNA-seq data for these genes when comparign QA and FA, with an R^2 of 0.8943 (P<0.01) (Fig. 12-B).

4. Discussion

4.1. Large-scale methylation examination of axillary buds with different flowering abilities

Flower bud formation is the essential prerequisite and yield foundation for fruit production in woody fruit trees (Albani and Coupland 2010; Chen *et al.* 2018). Numerous studies have reported the regulatory mechanisms of the flowering process throughout the plant life cycle, including floral induction (Wang *et al.* 2017), juvenile-to-adult transition (Huijser and Schmid 2011), reproduction (Han *et al.* 2019), and floral organ identity determination (Monniaux *et al.* 2017), which involve transcriptional, post-transcriptional, and epigenetic regulation across multiple flowering pathways. DNA methylation, as a key epigenetic modification, plays a critical role in floral induction and formation in woody plants such as apple (Xing *et al.* 2019a), pear (Wang *et al.* 2013), and citrus (Agustí *et al.* 2020). To date, genome-wide identification and analysis of DNA methylation and epigenetic variations in all sequence contexts in plants, i.e., *A. thaliana* (Zicola *et al.* 2019), rice (Xing M Q *et al.* 2015), and woody trees (Xing *et al.* 2019a), have confirmed their key regulatory functions in plant development and floral induction. In the current study, we compared DNA methylation between axillary buds of profusely flowering QA and non-flowering FA to elucidate the epigenetic changes associated with floral induction and formation in apple trees (Fig. 2). The methylation levels in axillary buds were 19.35, 62.96 and 17.68% for CG, CHG and CHH in FA, and 19.64, 62.49 and 17.86% for CG, CHG and CHH in QA (Fig. 1-A and B; Fig. 2-C), respectively, which is consistent with previous studies (Xing *et al.* 2019a) and suggests a correlation with the distinct flowering capacities of QA and FA.

The identification of DMRs between axillary buds of profusely flowering QA and non-flowering FA, along with functional analysis of these DMRs (Figs. 4 and 5), has provided an opportunity to uncover their key roles in multiple biological processes, such as floral induction and flowering. Similar findings have been reported in other studies regarding chromatin modifications (including DNA methylation) that contribute to regulating plant growth and reproductive development (Han *et al.* 2019; Xing *et al.* 2019a). Additionally, these DMRs between QA and FA were distributed across different gene regions with substantial variation, which is also an important factor influencing the transcription of related genes (Fig. 3). Indeed, DMRs occurring in various genomic regions (i.e., promoter, gene-body, or intron) can lead to differences in transcript levels in multiple plant species (Wang *et al.* 2017; Xing *et al.*

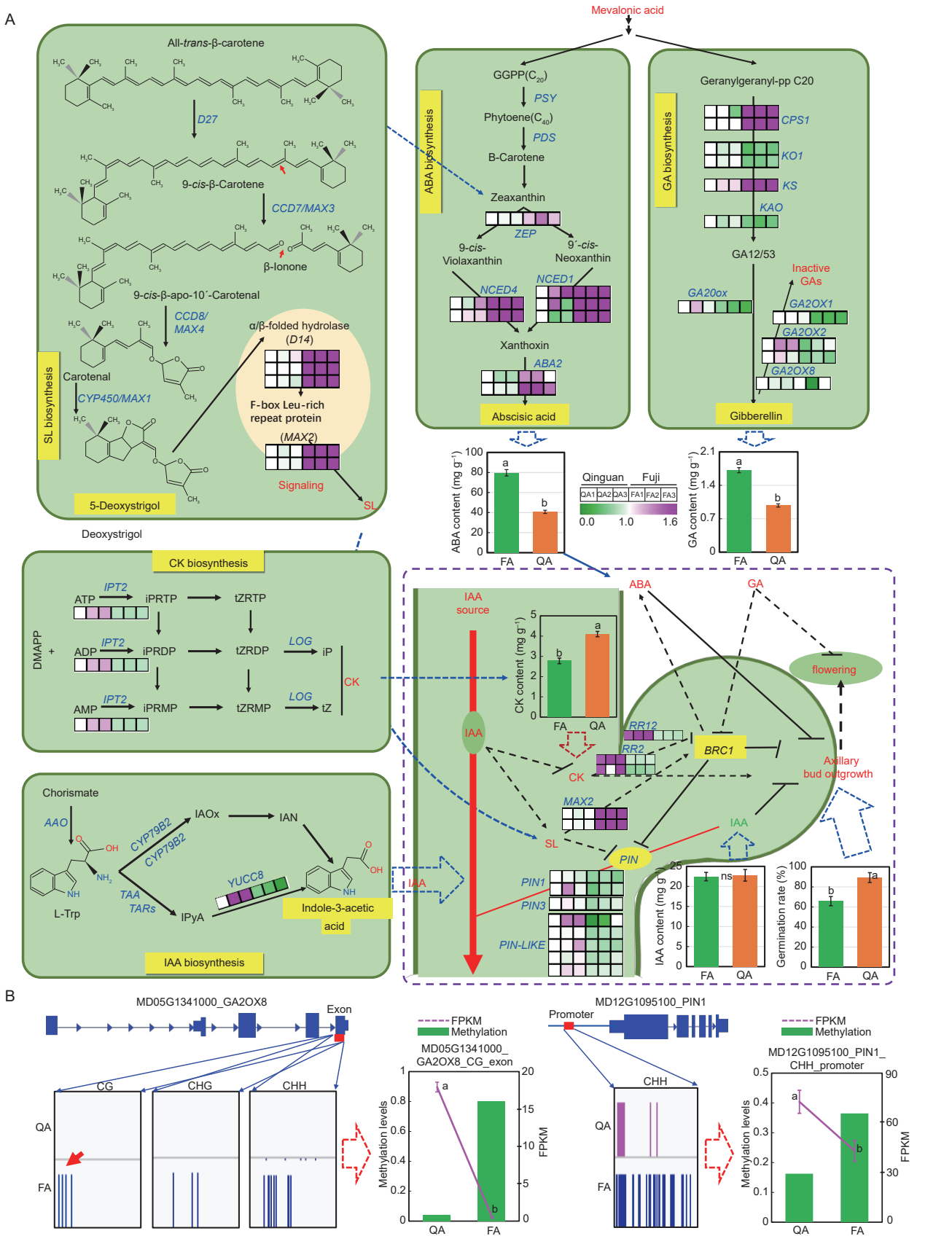


Fig. 11 The differentially methylated regions (DMRs) and differentially expressed genes (DEGs) involved in multiple hormone biosynthesis pathways contributed to the germination and outgrowth of axillary buds in 'Qinguan' (QA) and 'Fuji' (FA). A, the complex regulatory network involved in hormone biosynthesis and outgrowth of axillary bud. B, integrative genomics viewer snapshots of the DMRs, as well as the methylation and gene expression levels in the representative genes. Data are presented as the mean±standard error (n=3). The letters a and b indicate significant differences (P<0.05) and ns indicates a nonsignificant difference (P>0.05).

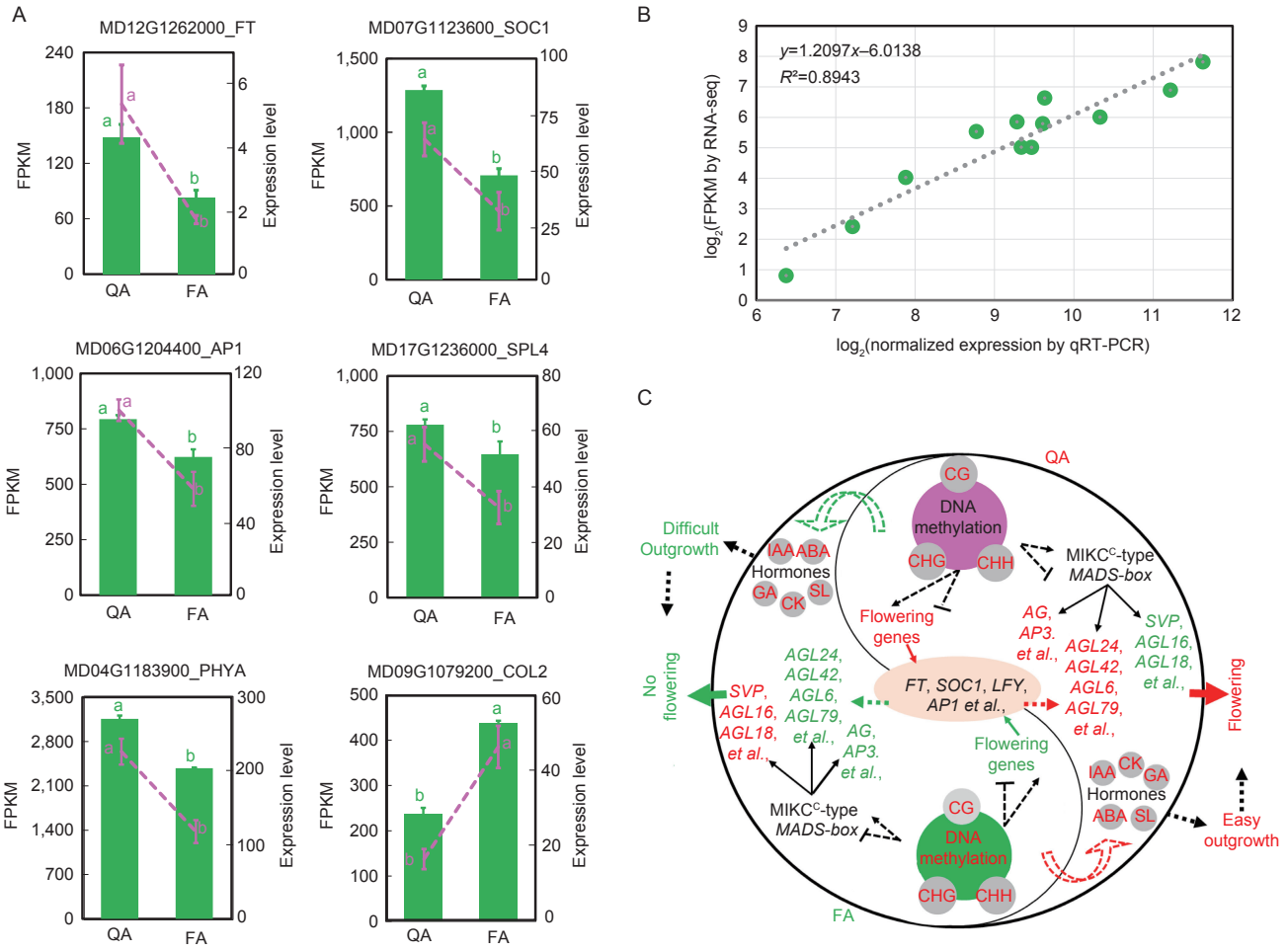


Fig. 12 The modeling of flowering regulatory mechanism in axillary buds of QA compared with FA. A, identification of related differentially expressed genes by qRT-PCR. B, linear relationship between qRT-PCR data and RNA-seq data. C, the modeling of flowering regulatory mechanism. The letters a and b indicate significant differences (P<0.05).

2019a), indicating that gene transcription is closely linked to methylation. In our data, we found that methylation levels were negatively correlated with gene expression levels in the gene-body region across CG, CHG, and CHH contexts (Fig. 6-A), but were positively correlated when methylation occurred in promoter regions in the CHH context (Fig. 6-B). This suggests that DNA methylation can play either a negative or positive role in regulating gene expression, depending on the gene region and the sequence context (CG, CHG or CHH). Similar results have been reported in other aspects of plants (Xing *et al.* 2019a).

4.2. Methylation levels change in multiple flowering pathway genes

Whether plants flower or not ultimately depends on the coordinated upregulation of key floral integrator genes (i.e., *FT*, *SOC1*, *SPLs*, *AP1* and *LEAFY*) involved in multiple flowering pathways under environmental and internal cues (Monniaux *et al.* 2017; Qin *et al.* 2017; Chahtane *et al.* 2018; Yao *et al.* 2019). For example, multi-layered regulation of *SPL15* and its cooperation with *SOC1* integrated gibberellin (GA) and age-related flowering pathways to regulate flowering at the SAM (Hyun *et al.* 2016). In our data, the key floral integrators (*FT*, *SOC1*, *SPLs*, *AP1* and *LEAFY*) were expressed significantly higher in axillary buds of profusely flowering QA than in non-flowering FA, which was associated with DNA methylation differences in various gene regions (Fig. 10). Additionally, previous studies have shown that the expression levels of these key flowering genes are significantly influenced by DNA methylation and other epigenetic variations in different gene regions (Xing *et al.* 2019a; Zicola *et al.* 2019; Agustí *et al.* 2020). For example, targeted DNA methylation represses the Block C enhancers of *FT* gene (located 5-kilobases (kb) upstream of the transcriptional start site), contributing to the regulation of floral transition under long-day photoperiods (Zicola *et al.* 2019). *SIN3-LIKE* genes mediate long-day induction of flowering through histone deacetylation to directly repress three *FT* repressors: *AP2* family transcription factors (Huang *et al.* 2019). Indeed, the upregulation of *FT* genes and downregulation of *AP2* genes in QA compared to FA (Fig. 12) were influenced by their DNA methylation patterns in different gene regions, contributing to axillary bud flowering in QA (Fig. 1) through epigenetic modification. Chromatin-dependent repression of floral integrator genes (*SOC1* and *FT*) by plant-specific PHD-containing proteins plays a key role in flowering regulation (Lopez-Gonzalez *et al.* 2014). Studies

have shown that *LFY* and *AP1* are conserved floral regulators in plants (Monniaux *et al.* 2017), and the floral transition is largely controlled by the meristem identity regulator *LEAFY*, which activates *APETALA1* (*AP1*) (Pastore *et al.* 2011). In summary, flowering in axillary buds of QA was largely determined by the expression of key flowering genes (i.e., *FT*, *SOC1*, *LEAFY* and *AP1*), which are significantly regulated by transcriptional and epigenetic mechanisms across multiple pathways.

In our data, the expression of MIKC^c subgroup *MADS-box* family genes differed significantly between QA and FA (Figs. 8 and 9), suggesting that they had a key role in flowering associated with epigenetic variations in different regions, similar results had been reported in other study (Rothkegel *et al.* 2017). For example, different *MADS-box* family genes, including floral regulators *FLC* and *SOC1*, directly regulate *SVP* gene expression and play a key role in floral transition through antagonistic chromatin modifications (Fernandez *et al.* 2014). NF-Y interacts with CONSTANS to directly regulate *SOC1* expression by modulating trimethylated H3K27 levels on its promoter, involving epigenetic regulation (Hou *et al.* 2014). Our data showed that multiple *NF-YA/B/C* family genes, as well as *SOC1*, were expressed at significantly higher levels in QA than in FA, accompanied by DNA methylation differences in various regions, contributing to the relatively higher flowering rate in QA axillary buds (Fig. 10). However, some *MADS-box* genes (i.e., *SVP*, *AGL15* and *AGL18* as floral repressors) showed the opposite pattern between QA and FA (Figs. 8 and 10). Indeed, even within the MIKC^c-type family, genes are subdivided into 14 monophyletic clades (i.e., *AGL6*, *SEP*, *AP1*, *SOC1*, *AP3/PI*, *SVP*, and *AGL15*) that play positive or negative regulatory roles in floral induction (Chen *et al.* 2017). *AGL15* and *AGL18*, together with *SVP*, are necessary to block the initiation of floral induction (Fernandez *et al.* 2014). *AGL15* repressed flowering by recruiting histone deacetylase complex components (SIN3/HDAC) (Hill *et al.* 2008). *SHORT VEGETATIVE PHASE* (*SVP*) is a key flowering regulator that repressed the *FT* and *SOC1* expression by binding to their regulatory sequences (Shen *et al.* 2011).

4.3. Changes in methylation levels of genes in multiple hormone pathways are associated with axillary bud flowering

High germination and outgrowth rates are essential for achieving at high flowering rate in many woody plants (Yang *et al.* 2016; Xing *et al.* 2019b). Phytohormone, including strigolactone (SL), auxin, cytokinin, abscisic acid (ABA), and gibberellin (GA), form an antagonistic or cooperative regulatory network that plays a key role in axillary bud outgrowth (Gonzalez-Grandio *et al.* 2013; Ni *et al.* 2015; Stes *et al.* 2015; Qiu *et al.* 2019; Shen *et al.* 2019). Our data showed that cytokinin (CK) levels and germination rates were significantly higher in axillary buds of profusely flowering QA than in non-flowering FA (Fig. 11), whereas ABA and GA levels showed the opposite pattern (Fig. 11), indicating that multiple hormones exert either negative or positive effects on axillary bud germination and flowering. Previous studies have shown that SLs repress axillary bud outgrowth through SL signaling genes (Stes *et al.* 2015; Wang *et al.* 2018). Consistent with this, genes involved in SL signaling (two *MAX2* and *three* D14) were significantly downregulated in axillary buds of profusely flowering QA compared to non-flowering FA, while genes in the strigolactone biosynthesis pathway showed no significant difference (Fig. 11). In strawberry, auxin and cytokinin exhibit contrasting behaviors in controlling axillary bud development and outgrowth (Qiu *et al.* 2019), and the Arabidopsis model indicates that high auxin levels inhibit axillary bud activity, whereas cytokinin has the opposite effect (Waldie and Leyser 2018). Among these hormones, auxin efflux *PIN* genes played a positively role in IAA-mediated axillary bud outgrowth by discharging transport of high auxin from the axillary bud meristem (Waldie and Leyser 2018; Qiu *et al.* 2019). Indeed, in the axillary bud meristem, eight *PIN* genes (i.e., two *PIN1*, one *PIN3*, and five *PIN-like*) were expressed significantly higher in QA than in FA (Fig. 11), corresponding to higher germination and flowering rates in QA axillary buds. This suggests that whether IAA is transported out of the axillary bud meristem is a key factor for bud outgrowth. Research has shown that *CsBRC1* inhibits axillary bud outgrowth by directly repressing *CsPIN3* expression in cucumber (Shen *et al.* 2019). Auxin transport mediated by *PIN1* also contributed to strigolactone-mediated shoot-branching control (van Rongen *et al.* 2019). Additionally, *BRC1* acts upstream of ABA in regulating axillary bud outgrowth by upregulating key ABA biosynthesis genes such as *NCED3*, leading to higher ABA levels (González-Grandío *et al.* 2013, 2016). A similar pattern was observed in our data: genes involved in ABA biosynthesis (three *NCED1*, two *NCED4*, one *ZEP*, and two *ABA2*) were upregulated in FA, which had a lower germination rate and no flowering, compared to QA, contributing to higher ABA levels in FA (Fig. 11). Moreover, studies have shown that GA plays a key role in regulating axillary bud outgrowth through interactions between DELLA and BRC1 proteins (Davière *et al.* 2014; Ni *et al.* 2015).

5. Conclusion

In summary, a multi-layered regulatory process — encompassing complex networks of key flowering genes, MIKC^c-type *MADS-box* genes, and phytohormone-mediated signaling pathways involved in axillary bud outgrowth — collectively contributes to floral induction in QA axillary buds of apple through DNA methylation and other epigenetic modifications (Fig. 12-C).

Acknowledgements

This work was supported by the National Natural Science Foundation of China (32472668 and 32072522).

Declaration of competing interest

The authors declare that they have no conflict of interest.

Declaration of generative AI and AI-assisted technologies in the writing process

The authors declare that they did not use AI in the preparation

and writing of this manuscript.

Appendices associated with this paper are available at https://doi.org/10.1016/j.jia.2025.12.065

References

Abdel-Latif A, Osman G. 2017. Comparison of three genomic DNA extraction methods to obtain high DNA quality from maize. *Plant Methods*, **13**, 1.

Agustí M, Mesejo C, Muñoz-Fambuena N, Vera-Sirera F, de Lucas M, Martínez-Fuentes A, Reig C, Iglesias D J, Primo-Millo E, Blázquez M A. 2020. Fruit-dependent epigenetic regulation of flowering in *Citrus*. *New Phytologist*, **225**, 376–384.

Albani M C, Coupland G. 2010. Comparative analysis of flowering in annual and perennial plants. *Current Topics in Developmental Biology*, **91**, 323–348.

Amasino R M, Michaels S D. 2010. The timing of flowering. *Plant Physiology*, **154**, 516–520.

Anders S, Huber W. 2010. Differential expression analysis for sequence count data. *Genome Biology*, **11**, R106.

Andrés F, Coupland G. 2012. The genetic basis of flowering responses to seasonal cues. *Nature Reviews Genetics*, **13**, 627.

Chahtane H, Zhang B, Norberg M. 2018. LEAFY activity is post-transcriptionally regulated by *BLADE ON PETIOLE2* and *CULLIN3* in *Arabidopsis*. *New Phytologist*, **220**, 2.

Chen F, Zhang X, Liu X, Zhang L. 2017. Evolutionary analysis of MIKC^c-type MADS-box genes in gymnosperms and angiosperms. *Frontiers in Plant Science*, **8**, 895.

Chen X, Qi S, Zhang D, Li Y, An N, Zhao C, Zhao J, Shah K, Han M, Xing L. 2018. Comparative RNA-sequencing-based transcriptome profiling of buds from profusely flowering QA and weakly flowering 'Nagafu no. 2' apple varieties reveals novel insights into the regulatory mechanisms underlying floral induction. *BMC Plant Biology*, **18**, 370.

Daccord N, Celton J M, Linsmith G, Becker C, Choisne N, Schijlen E, van de Geest H, Bianco L, Micheletti D, Velasco R, Di Pierro E A, Gouzy J, Rees D J G, Guérif P, Muranty H, Durel C E, Laurens F, Lespinasse Y, Gaillard S, Aubourg S, *et al.* 2017. High-quality *de novo* assembly of the apple genome and methylome dynamics of early fruit development. *Nature Genetics*, **49**, 1099–1106.

Davière J M, Wild M, Regnault T, Baumberger N, Eisler H, Genschik P, Achard P. 2014. Class I TCP-DELLA interactions in inflorescence shoot apex determine plant height. *Current Biology*, **24**, 1923–1928.

Djilianov D L, Dobrev P I, Moyankova D P, Vankova R, Georgieva D T, Gajdošová S, Motyka V. 2013. Dynamics of endogenous phytohormones during desiccation and recovery of the resurrection plant species *Haberlea rhodopensis*. *Journal of Plant Growth Regulation*, **32**, 564–574.

Dobrev P I, Vankova R. 2012. Quantification of abscisic acid, cytokinin, and auxin content in salt-stressed plant tissues. In: *Plant Salt Tolerance*. Springer, Berlin, Germany. pp. 251–261.

Dorca-Fornell C, Gregis V, Grandi V, Coupland G, Colombo L, Kater MM. 2011. The *Arabidopsis* SOC1-like genes *AGL42*, *AGL71* and *AGL72* promote flowering in the shoot apical and axillary meristems. *The Plant Journal*, **67**, 1006–1017.

Du Z, Zhou X, Ling Y, Zhang Z, Su Z. 2010. agriGO: A GO analysis toolkit for the agricultural community. *Nucleic Acids Research*, **38**, W64–W70.

Huang F, Yuan W Y, Tian S, Zheng Q J, He Y H. 2019. *SIN3 LIKE* genes mediate long-day induction of flowering but inhibit the floral transition in short days through histone deacetylation in Arabidopsis. *The Plant Journal*, **100**, 101–113.

FAO. 2023. FAOSTAT. [2023-6-1]. http://www.fao.org/faostat

Feng H, Conneely K N, Wu H. 2014. A Bayesian hierarchical model to detect differentially methylated loci from single nucleotide resolution sequencing data. *Nucleic Acids Research*, **42**, e69.

Fernandez D E, Wang C T, Zheng Y, Adamczyk B J, Singhal R, Hall P K, Perry S E. 2014. The MADS-domain factors *AGAMOUS-LIKE15* and *AGAMOUS-LIKE18*, along with *SHORT VEGETATIVE PHASE* and *AGAMOUS-LIKE24*, are necessary to block floral gene expression during the vegetative phase. *Plant Physiology*, **165**, 1591–1603.

Gallusci P, Hodgman C, Teyssier E, Seymour G B. 2016. DNA methylation and chromatin regulation during fleshy fruit development and ripening. *Frontiers in Plant Science*, **7**, 807.

González-Grandío E, Pajoro A, Franco-Zorrilla JM, Tarancón C, Cubas P. 2016. Abscisic acid signaling is controlled by a *BRANCHED1/HD-ZIP I* cascade in *Arabidopsis* axillary buds. *Proceedings of the National Academy of Sciences of the United States of America*, **114**, 201613199.

González-Grandío E, Poza-Carrion C, Sorzano COS, Cubas P. 2013. BRANCHED1 promotes axillary bud dormancy in response to shade in *Arabidopsis*. *Plant Cell*, **25**, 834–850.

Haberman A, Ackerman M, Crane O, Kelner JJ, Costes E, Samach A. 2016. Different flowering response to various fruit loads in apple cultivars correlates with degree of transcript reaccumulation of a TFL1-encoding gene. *Plant Journal*, **87**, 161–173.

Han Q, Bartels A, Cheng X, Meyer A, An Y Q C, Hsieh T F, Xiao W. 2019. Epigenetics regulates reproductive development in plants. *Plants*, **8**, 564.

He Y. 2015. Enabling photoperiodic control of flowering by timely chromatin silencing of the florigen gene. *Nucleus*, **6**, 179–182.

Hill K, Wang H, Perry S E. 2008. A transcriptional repression motif in the MADS factor *AGL15* is involved in recruitment of histone deacetylase complex components. *Plant Journal*, **53**, 172–185.

Hou X, Zhou J, Liu C, Liu L, Shen L, Yu H. 2014. Nuclear factor Y-mediated H3K27me3 demethylation of the *SOC1* locus orchestrates flowering responses of *Arabidopsis*. *Nature Communications*, **5**, 4601.

Huijser P, Schmid M. 2011. The control of developmental phase transitions in plants. *Development*, **138**, 4117–4129.

Hyun Y, Richter R, Vincent C, Martinez-Gallegos R, Porri A, Coupland G. 2016. Multi-layered regulation of *SPL15* and cooperation with *SOC1* integrate endogenous flowering pathways at the *Arabidopsis* shoot meristem. *Developmental Cell*, **37**, 254–266.

Jeong J H, Song H R, Ko J H, Jeong Y M, Kwon Y E, Seol J H, Amasino R M, Noh B, Noh Y S. 2009. Repression of *FLOWERING LOCUS T* chromatin by functionally redundant histone H3 lysine 4 demethylases in *Arabidopsis*. *PLoS ONE*, **4**, e8033.

Jung C. 2017. Flowering time regulation: Agrochemical control of flowering. *Nature Plants*, **3**, 17045.

Kanehisa M, Sato Y, Kawashima M, Furumichi M, Tanabe M. 2016. KEGG as a reference resource for gene and protein annotation. *Nucleic Acids Research*, **44**, D457–D462.

Kim J Y, Oh J E, Noh Y S, Noh B. 2015. Epigenetic control of juvenile-to-adult phase transition by the *Arabidopsis* SAGA-like complex. *The Plant Journal*, **83**, 537–545.

Krueger F, Andrews S R. 2011. Bismark: A flexible aligner and methylation caller for Bisulfite-Seq applications. *Bioinformatics*, **27**, 1571–1572.

Li D, Zhang H, Mou M, Chen Y, Xiang S, Chen L, Yu D. 2019. *Arabidopsis* class II TCP transcription factors integrate with the FT–FD module to control flowering. *Plant Physiology*, **181**, 97–111.

Li R, Yu C, Li Y, Lam T W, Yiu S M, Kristiansen K, Wang J. 2009. SOAP2: An improved ultrafast tool for short read alignment. *Bioinformatics*, **25**, 1966–1967.

Liu R, How-Kit A, Stammitti L, Teyssier E, Rolin D, Mortain-Bertrand A, Halle S, Liu M, Kong J, Wu C, Degraeve-Guibault C, Chapman N H, Maucourt M, Hodgman T C, Tost J, Bouzayen M, Hong Y, Seymour G B, Giovannoni J J, Gallusci P. 2015. A DEMETER-like DNA demethylase governs tomato fruit ripening. *Proceedings of the National Academy of Sciences of the United States of America*, **112**, 10804–10809.

Lopez-Gonzalez L, Mouriz A, Narro-Diego L, Bustos R, Martinez-Zapater J M, Jarillo J A, Pineiro M. 2014. Chromatin-dependent repression of the *Arabidopsis* floral integrator genes involves plant specific PHD-containing proteins. *Plant Cell*, **26**, 3922–3938.

Meijón M, Cañal M J, Valledor L, Rodríguez R, Feito I. 2011. Epigenetic and physiological effects of gibberellin inhibitors and chemical pruners on the floral transition of azalea. *Physiologia Plantarum*, **141**, 276–288.

Monniaux M, Mckim S M, Cartolano M, Thévenon E, Parcy F, Tsiantis M, Hay A. 2017. Conservation vs divergence in LEAFY and APETALA1 functions between *Arabidopsis thaliana* and *Cardamine hirsuta*. *New Phytologist*, **216**, 549–561.

Mortazavi A, Williams B A, McCue K, Schaeffer L, Wold B. 2008.

Mapping and quantifying mammalian transcriptomes by RNA-Seq. *Nature Methods*, **5**, 621–628.
Narsai R, Secco D, Schultz M D, Ecker J R, Lister R, Whelan J. 2017. Dynamic and rapid changes in the transcriptome and epigenome during germination and in developing rice (*Oryza sativa*) coleoptiles under anoxia and re-oxygenation. *The Plant Journal*, **89**, 805–824.
Ni J, Gao C, Chen M S, Pan B Z, Xu Z F. 2015. Gibberellin promotes shoot branching in the perennial woody plant *Jatropha curcas*. *Plant and Cell Physiology*, **56**, 1655–1666.
Park Y, Wu H. 2016. Differential methylation analysis for BS-seq data under general experimental design. *Bioinformatics*, **32**, 1–10.
Pastore J J, Limpuangthip A, Yamaguchi N, Wu M F, Sang Y, Han S K, Malaspina L, Chavdaroff N, Yamaguchi A, Wagner D. 2011. *LATE MERISTEM IDENTITY2* acts together with *LEAFY* to activate *APETALA1*. *Development*, **138**, 3189–3198.
Pazhouhandeh M, Molinier J, Berr A, Genschik P. 2011. *MSI4/FVE* interacts with *CUL4-DDB1* and a PRC2-like complex to control epigenetic regulation of flowering time in *Arabidopsis*. *Proceedings of the National Academy of Sciences of the United States of America*, **108**, 3430–3435.
Qin Z, Wu J, Geng S, Feng N, Chen F, Kong X, Song G, Chen K, Li A, Mao L, Wu L. 2017. Regulation of FT splicing by an endogenous cue in temperate grasses. *Nature Communications*, **8**, 14320.
Qiu Y, Guan SC, Wen C, Li P, Gao Z, Chen X. 2019. Auxin and cytokinin coordinate the dormancy and outgrowth of axillary bud in strawberry runner. *BMC Plant Biology*, **19**, 528.
van Rongen M, Bennett T, Ticchiarelli F, Leyser O. 2019. Connective auxin transport contributes to strigolactone-mediated shoot branching control independent of the transcription factor *BRC1*. *PLoS Genetics*, **15**, e1008023.
Rothkegel K, Sánchez E, Montes C, Greve M, Tapia S, Bravo S, Prieto H, Almeida A M. 2017. DNA methylation and small interference RNAs participate in the regulation of MADS-box genes involved in dormancy in sweet cherry (*Prunus avium* L.). *Tree Physiology*, **37**, 1739–1751.
Sacharowski S P, Gratkowska D M, Sarnowska E A, Kondrak P, Jancewicz I, Porri A, Bucior E, Rolicka A T, Franzen R, Kowalczyk J. 2015. SWP73 subunits of Arabidopsis SWI/SNF chromatin remodeling complexes play distinct roles in leaf and flower development. *Plant Cell*, **27**, 1889–1906.
Sánchez-Taltavull D, Ramachandran P, Lau N, Perkins T J. 2016. Bayesian correlation analysis for sequence count data. *PLoS ONE*, **11**, e0163595.
Seymour G, Poole M, Manning K, King G J. 2008. Genetics and epigenetics of fruit development and ripening. *Current Opinion in Plant Biology*, **11**, 58–63.
Shen J, Zhang Y, Ge D, Wang Z, Song W, Gu R, Che G, Cheng Z, Liu R, Zhang X. 2019. *CsBRC1* inhibits axillary bud outgrowth by directly repressing the auxin efflux carrier *CsPIN3* in cucumber. *Proceedings of the National Academy of Sciences of the United States of America*, **116**, 17105–17114.
Shen L, Kang Y G G, Liu L, Yu H. 2011. The J-domain protein J3 mediates the integration of flowering signals in *Arabidopsis*. *Plant Cell*, **23**, 499–514.
Smaczniak C, Immink R G H, Angenent G C, Kaufmann K. 2012. Developmental and evolutionary diversity of plant MADS-domain factors: Insights from recent studies. *Development*, **139**, 3081–3098.
Stes E, Depuydt S, De Keyser A, Matthys C, Audenaert K, Yoneyama K, Werbrouck S, Goormachtig S, Vereecke D. 2015. Strigolactones as an auxiliary hormonal defence mechanism against leafy gall syndrome in *Arabidopsis thaliana*. *Journal of Experimental Botany*, **66**, 5123–5134.
Waldie T, Leyser O. 2018. Cytokinin targets auxin transport to promote shoot branching. *Plant Physiology*, **177**, 803–818.
Wang B, Smith S M, Li J. 2018. Genetic regulation of shoot architecture. *Annual Review of Plant Biology*, **69**, 437–468.
Wang L, Kong D, Lv Q, Niu G Q, Han T, Zhao X, Meng S, Cheng Q, Guo S, Du J. 2017. Tetrahydrofolate modulates floral transition through epigenetic silencing. *Plant Physiology*, **174**, 1274–1284.
Wang Z, Meng D, Wang A, Li T, Jiang S, Cong P, Li T. 2013. The methylation of the PcMYB10 promoter is associated with green-skinned sport in max red bartlett pear. *Plant Physiology*, **162**, 885–896.
Wu H, Xu T, Feng H, Chen L, Li B, Yao B, Qin Z, Jin P, Conneely K N. 2015. Detection of differentially methylated regions from whole-genome bisulfite sequencing data without replicates. *Nucleic Acids Research*, **43**, e141.
Xing L, Li Y, Qi S, Zhang C, Ma W, Zuo X, Liang J, Gao C, Jia P, Shah K, Zhang D, An N, Zhao C, Han M, Zhao J. 2019a. Comparative RNA-sequencing and DNA methylation analyses of apple (*Malus domestica* Borkh.) buds with diverse flowering capabilities reveal novel insights into the regulatory mechanisms of flower bud formation. *Plant Cell Physiology*, **60**, 1702–1721.
Xing L, Zhang D, Qi S, Chen X, An N, Li Y, Zhao C, Han M, Zhao J. 2019b. Transcription profiles reveal the regulatory mechanisms of spur bud changes and flower induction in response to shoot bending in apple (*Malus domestica* Borkh.). *Plant Molecular Biology*, **99**, 45–66.
Xing L, Zhang D, Song X, Weng K, Shen Y, Li Y, Zhao C, Ma J, An N, Han M. 2016a. Genome-wide sequence variation identification and floral-associated trait comparisons based on the re-sequencing of the 'Nagafu No. 2' and QA varieties of apple (*Malus domestica* Borkh.). *Frontiers in Plant Science*, **7**, 908.
Xing L, Zhang D, Zhao C, Li Y, Ma J, An N, Han M. 2016b. Shoot bending promotes flower bud formation by miRNA-mediated regulation in apple (*Malus domestica* Borkh.). *Plant Biotechnology Journal*, **14**, 749–770.
Xing L B, Zhang D, Li Y M, Shen Y W, Zhao C P, Ma J J, An N, Han M Y. 2015. Transcription profiles reveal sugar and hormone signaling pathways mediating flower induction in apple (*Malus domestica* Borkh.). *Plant and Cell Physiology*, **56**, 2052–2068.
Xing M Q, Zhang Y J, Zhou S R, Hu W Y, Wu X T, Ye Y J, Wu X X, Xiao Y P, Li X, Xue H W. 2015. Global analysis reveals the crucial roles of DNA methylation during rice seed development. *Plant Physiology*, **168**, 1417–1432.
Xu J, Xu H, Xu Q, Deng X. 2015. Characterization of DNA methylation variations during fruit development and ripening of sweet orange. *Plant Molecular Biology Reporter*, **33**, 1–11.
Xu M, Hu T, Smith M R, Poethig R S. 2016. Epigenetic regulation of vegetative phase change in *Arabidopsis*. *The Plant Cell*, **28**, 28–41.
Yang W, Pallas B, Durand J B, Martinez S, Han M, Costes E. 2016. The impact of long-term water stress on tree architecture and production is related to changes in transitions between vegetative and reproductive growth in the 'Granny Smith' apple cultivar. *Tree Physiology*, **36**, 1369–1381.
Yao T, Park B S, Mao H Z, Seo J S, Ohama N, Li Y, Yu N, Mustafa N F B, Huang C H, Chua N H. 2019. Regulation of flowering time by *SPL10/MED25* module in *Arabidopsis*. *New Phytologist*, **224**, 493–504.
Zhao T, Holmer R, de Bruijn S, Angenent G C, van den Burg H A, Schranz M E. 2017. Phylogenomic synteny network analysis of MADS-box transcription factor genes reveals lineage-specific transpositions, ancient tandem duplications, and deep positional conservation. *Plant Cell*, **29**, 1278–1292.
Zicola J, Liu L Y, Tänzler P, Turck F. 2019. Targeted DNA methylation represses two enhancers of FLOWERING LOCUS T in *Arabidopsis thaliana*. *Nature Plants*, **5**, 300–307.

Executive Editor-in-Chief Sanwen Huang
Managing Editor Lingyun Weng